ACS APPLIED MATERIALS & INTERFACES

www.acsami.org

Review

Research Progress in 3D Printed Biobased and Biodegradable Polyester/Ceramic Composite Materials: Applications and Challenges in Bone Tissue Engineering

Shunshun Zhu, Hongnan Sun,* Taihua Mu,* and Aurore Richel

Cite This: https://doi.org/10.1021/acsami.4c15719

Read Online

ACCESS | Metrics & More | Article Recommendations

ABSTRACT: Transplantation of bone implants is currently recognized as one of the most effective means of treating bone defects. Biobased and biodegradable polyester composites combine the good mechanical and degradable properties of polyester, thereby providing an alternative for bone implant materials. Bone tissue engineering (BTE) accelerates bone defect repair by simulating the bone microenvironment. Composite scaffolds support bone formation and further accelerate the process of bone repair. The introduction of 3D printing technology enables the preparation of scaffolds to be more precise, reproducible, and flexible, which is a very promising development. This review presents the physical properties of BTE scaffolds and summarizes the strategies adopted by domestic and international scholars to improve the properties of scaffolds based on biobased and biodegradable polyester/ceramic composites in recent years. In addition, future development prospects in the field and the challenges of expanding production in clinical applications are presented.

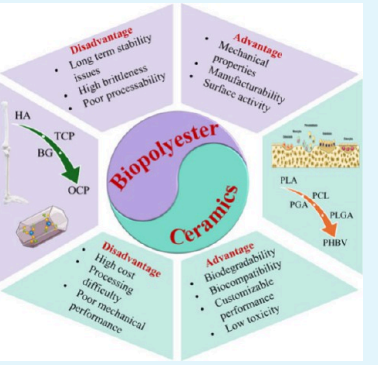

KEYWORDS: *polyester, ceramic, 3D printing, functional nanomaterials, bone tissue engineering scaffolds, bone defect regeneration*

1. INTRODUCTION

With the change in modern dietary structure, an aging population, and an accelerated pace of social life, orthopedic diseases, such as bone fractures, bone tumors, and osteoporosis, have gradually become one of the most important problems affecting human health. Middle-aged and elderly people have serious bone health problems, with a prevalence rate of 32% among people over 65 years of age.[1] The strength of bones decreases as humans age, and their associated defects and diseases become more prominent with age. Although bones have their own healing/regenerative ability to repair small bone defects, large-sized bone defects caused by accidents, bone tumor removal, or injuries are not easily healed by the bone itself. When a bone defect exceeds 6 cm, it cannot heal itself.[2] One of the methods of healing large defects is the use of autogenous bone grafting.[3,4] This approach has limitations, including high donor site morbidity, limited numbers, and secondary injury. In addition, patients facing major bone defects caused by severe trauma or infectious disease rely on the surgical implantation of an exogenous bone graft for complete recovery. According to statistics, the number of bone transplantation operations performed worldwide each year exceeds 2.2 million, with a total cost as high as US$ 2.5 billion.[5] However, traditional bone implants, such as metal and allogeneic bone, face challenges like the need for secondary surgery,[6,7] potential immunogenicity, and other issues (Table 1), which further aggravate the risk of bone repair surgery. As a result, researchers in different fields have been exploring alternative methods to heal large bone defects and have developed tissue engineering (TE) techniques, which are now widely used in the biomedical field (Figure 1). As the field of TE continues to be researched and developed, it has become an area of interest in repairing skeletal defects for more effective and predictable medical practice in the future.

Bones are mainly composed of long bones (composed of diaphysis, epiphysis, and metaphysis), flat bone (such as skull and scapula), periosteum, and medullary cavity. According to the function, it can be divided into load-bearing bone (such as the femur) and protective bone (such as the skull). The microstructure is divided into bone matrix, osteon, cells (osteoblasts, osteoclasts, osteocytes, osteoprogenitors cells, etc.), blood vessels and nerves, trabeculae, etc.[8,9] In the process of growth, repair, and adaptation to external mechanical stress, bone is driven by the dynamic balance of osteogenesis and osteoclast, which is a biological process to maintain the dynamic balance of bone tissue.[10] The core of bone remodeling is the coupling of osteogenesis and osteoclast

Received: September 13, 2024
Revised: December 25, 2024
Accepted: December 25, 2024

Table 1. Comparison of Properties of Typical Bone Implant Materials

	Type	Advantage	Disadvantage	Ref
Natural bone implant	Autogenous bone	Osteogenic activity, good biocompatibility	Long operation time and limited bone supply	(2)
	Homologous bone	Wide material source, good biocompatibility	Immune response, no bone activity, poor mechanical stability	(3)
	Metatarsal bone	Low-cost, widely available	No immunogenicity, no bone activity	(4)
Metal	Tantalum, titanium, magnesium alloy	Lightweight, high strength, good biocompatibility	The production process is complex, bone formation is slow, and nondegradable	(5)
Ceramic	β-tricalcium phosphate (β-TCP)	Like bone mineral component, good degradability, osteogenic activity, compressive property	Mechanical brittleness	(10)
	BG			
	HA			
Polyester	PLA	Good plasticity, biocompatibility, and biodegradability	Insufficient mechanical properties, leading to osteoporosis	(11)
	PCL			
	PGA			
	PLGA			
Complex	PLA/HA	Like natural bone matrix, good biocompatibility, good bone conductivity, low immunogenicity	The rigors of the manufacturing process	(12)

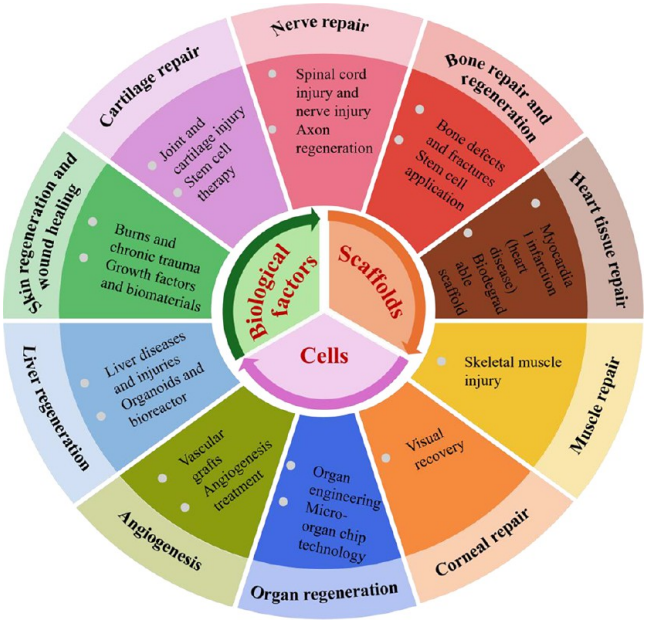

Figure 1. Application of tissue engineering in repairing damaged body tissues.

activity. In the repair of bone injury and microfracture, osteoclasts first remove damaged or old bone tissue, and then osteoblasts fill new bone.[11] The imbalance between osteogenesis and osteoclast activity may lead to osteopetrosis (insufficient osteoclast) or osteoporosis (insufficient osteogenesis). Based on that, bone tissue engineering (BTE) can help restore balance by providing physical support, guiding cell behavior, and regulating the microenvironment. BTE simulates bone structure to provide a microenvironment suitable for host cell proliferation, differentiation, and new bone tissue reconstruction, thereby accelerating the repair of bone defects (Figure 2). BTE scaffolds are a good choice for simulating cancellous bone structure.[12,13] The ideal scaffold for BTE should possess a series of key properties, such as good mechanical properties, appropriate porosity, surface roughness, biodegradability, and osteogenic activity (Table 2). Biocompatibility is a key consideration to ensure that the material does not provoke adverse immune responses or toxicity. Combining biocompatible materials with the appropriate fabrication techniques is essential to establish the preparation of optimal bone scaffolds.

Biobased and biodegradable polyesters, such as polylactic acid (PLA), D-poly lactic acid (PDLA), polycaprolactone (PCL), and polyglycolic acid (PGA), have attracted extensive attention in bone repair applications due to their excellent

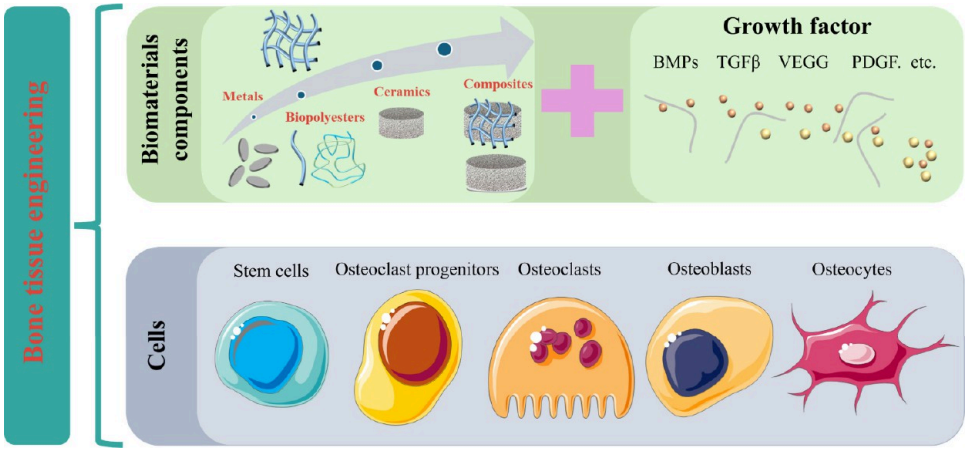

Figure 2. Scheme representing the synthetic bone graft for bone tissue regeneration.

https://doi.org/10.1021/acsami.4c15719
ACS Appl. Mater. Interfaces XXXX, XXX, XXX−XXX

Table 2. Biological Design Properties of Bone Tissue Scaffolds

Factor		Principle	Ref
Biocompatibility	Material composition	Carboxy, sulfonate, amino, amide, and imino groups facilitate cell adhesion and proliferation.	(14)
	Topology	The topological structure of biological implants, such as surface roughness, porosity and distribution, groove size, and orientation, greatly influences cell adhesion behavior.	(15)
	Hydrophilicity	Strongly hydrophilic surfaces are unfavorable for protein adsorption and cell adhesion.	(16)
	Tissue reactivity	Physiological substances surrounding bone tissue contain chloride ions, dissolved oxygen, proteins, fats, organic acids, enzymes, etc., which can react with certain materials, causing inflammation and abnormal cell differentiation.	(17)
	Mechanical properties	Bone repair materials require strength, toughness, hardness, and Young's modulus compatible with human bone tissue.	(18)
	Biodegradability	Biodegradable matrix materials can form channels for recruited cells to migrate from the surface of the material to the interior of the cell during degradation. The degradation rate of the material should match the endogenous cellular matrix secretion capacity.	(19)
Bone tissue-induced regenerative properties	Seductive	Large pores of 100−500 μm provide space for bone tissue growth and act as osteoconductors, while the micropores of 1−10 μm facilitate osmosis, circulation, and nutrient supply.	(20)
	Conductivity	The ability of implanted materials to induce differentiation of mesenchymal cells to osteoblasts.	(21)

biodegradability and biocompatibility. These materials have been approved as biomedical materials by multiple regulatory agencies. They can be degraded step by step *in vivo* without residue, irritation, or toxic side effects. The degradation rate and mechanical properties of these biopolyesters can be altered by adjusting the molecular weight and modifying the polymerization and molding methods. However, there are still some problems with biopolyesters, such as individual polyester materials having low mechanical strength, and the acidic products produced by their degradation may hinder the growth of tissues and cells. Ceramic has excellent mechanical properties and can slowly release Ca^{2+} and PO_4^{3-} during degradation due to its similarity to the components of the inorganic phase of human bones (most of which are hydroxyapatite-HA crystals), thus providing an important raw material for bone reconstruction.[10] In addition, the degradation of the ceramic can neutralize H^+ generated by the degradation of the polyester to further reduce the probability of inflammatory reaction, so the bone implant prepared by the biopolyester/ceramic composite material exhibits excellent bone repair effect.[11]

At present, the preparation pathways of biopolyester/ceramic composite scaffolds mainly include electrostatic spinning,[22,23] gas foaming,[24,25] solvent-casting particulate leaching (SCPL),[26] and thermally induced phase separation (TIPS)[27−29] (Table 3). However, the scaffolds obtained by these methods usually have irregular structures, uncontrollable pore sizes, relatively low strength, and poor repeatability, thereby reducing the practicability of the scaffold. The three-dimensional (3D) printing technique significantly improves the limitations of conventional scaffold fabrication. This technique was first reported in 1989[30] and has been rapidly and widely used in the field of scaffold molding. It is also known as additive material manufacturing and quickly and accurately creates solid models of BTE scaffolds based on the principles of layered manufacturing and layer-by-layer stacking through computer aided design (CAD) and numerical control technology.[31] Biopolyester/ceramic composites have good moldability and can be used as the raw material for 3D printing, offering a new method for preparing BTE scaffolds.[32,33] 3D printing technologies, such as bioprinting technologies, including droplet ejection printing (Figure 3a), pneumatic extrusion printing (Figure 3b), mechanical extrusion printing (Figure 3c), thermal inject printing (Figure 3d), piezoelectric inject printing (Figure 3e), laser-based printing (Figure 3f),[34] fused deposition modeling (FDM) (Figure 3g),[35,36] scanning laser sintering (SLS) (Figure 3h),[37] stereolithography printing (SLA) (Figure 3i),[38,39] and digital light processing (DLP) (Figure 3j),[40] have made the preparation of biopolyester/ceramic scaffolds more accurate, efficient, and repeatable (Table 4). The bone scaffold manufactured using this technology can simulate the bone structure of a bone defect part in a patient, and the pore diameter inside the scaffold can be accurately regulated and controlled, so that the technology has attracted wide attention in the field of preparation of biobased and biodegradable polyester/ceramic tissue engineering scaffolds.

2. BIOBASED AND BIODEGRADABLE POLYESTERS/CERAMIC

2.1. Biobased and Biodegradable Polyesters. Biopolyester materials were first put into the medical industry in the 1930s, initially applied as materials for external wounds or sutures. The biopolyesters used for bone repair mainly include PLA, PCL, PGA, polylactic-*co*-glycolic acid (PLGA), poly(hydroxybutyrate) (PHB), poly(citrate sebacate) (PCS), polypropylene fumarate (PPF), polyActive, poly(propylene carbonate) (PPC), and others.[42,43] The synthesis methods and physicochemical properties of common biopolyesters are summarized in Table 5 and Figure 4.

2.1.1. PLA. PLA is a thermoplastic polyester condensed from lactic acid and has great potential as a biobased and biodegradable bone repair material due to its good mechanical strength, biodegradability, and biocompatibility.[44,45] PLA is an optically active polymer, which can be divided into L-poly(lactic acid) (PLLA)[46] and PDLA.[47] They have different physical properties and different degradation rates. PLA has excellent biodegradability, and PLA and its products degrade in the natural environment after being discarded and eventually decompose into carbon dioxide (CO_2) and water. In addition to its environmental characteristics, PLA has good strength, making it easy to process, and it also has transparency and gloss, which are rare in other degradable plastics. At the same time, PLA has excellent hydrophobicity due to its ester group and is commonly used in biomedical materials.[48,49] However, PLA has some weaknesses, such as rapid degradation, with intermediate products accumulating locally, leading to a low pH value.

2.1.2. PCL. PCL has good biocompatibility, high flexibility, and high elongation and produces fewer acidic breakdown

https://doi.org/10.1021/acsami.4c15719
ACS Appl. Mater. Interfaces XXXX, XXX, XXX−XXX

Table 3. Preparation Methods of Bone Tissue Engineering Scaffolds

Preparation method	Preparation principle	Advantage	Disadvantage	Ref
Electrostatic spinning	The polymer solution or molten substance is stretched into nanoscale or micron-scale fine fibers by a high-voltage electric field, and then these fibers are deposited into a scaffold	Standard method for fabricating nanofibrous scaffolds	Toxic solvents are used; fabricating a 3D structure with required pore sizes is difficult	(22, 23)
Gas foaming	An inert gas is used as a foaming agent to create pressure within the polymers in solvents under high temperatures. The pressure from the gas is exerted until it reaches saturation, forming gas bubbles that create the porous structure	High porosity, small pore size, and no use of organic solvent	Narrow pore size distribution of vesicles	(24, 25)
Solvent casting/particle leaching	Removing the solvent from the polymer and filtering to obtain a porous structure	High porosity, low cost	Toxic nature, time-intensive	(26)
Thermally induced phase separation	The polymer dissolves in the solvent at a higher temperature, and the porous structure is formed by lowering the temperature	High porosity with a high surface-volume ratio	Can only be used for thermoplastics	(27−29)
Bioprinting	Technology for manufacturing brackets by means of layer-by-layer material accumulation based on 3D CAD data	High printing speed, supports printing scaffolds with high cell viability	Dependent on the existence of cells	(30)

products.[50,51] Although PCL degrades more slowly than other polyesters, such as PLA, this provides ample time for bone remodeling in patients. In addition, PCL has a melting temperature of 55−60 °C and good processability.[52] However, the mechanical properties of PCL are relatively low, and the degradation rate and efficiency are closely related to environmental conditions.[53]

2.1.3. PGA. PGA is a polymer with high crystallinity and an excellent tensile strength and modulus. PGA can be hydrolyzed and degraded into small nontoxic molecules (such as glycolic acid), and the degradation products are easily absorbed by human metabolism, making it a biocompatible material. PGA can be used to prepare medical materials such as bioabsorbable sutures, slow-release drug carriers, and fracture fixators, reducing the risk of secondary surgery and being suitable for scenarios requiring high strength.[54] However, it has high brittleness, poor toughness, and is prone to brittle fracture.[12,55] The degradation rate of PGA is fast in humid environments, making it unsuitable for long-term application.

2.1.4. PLGA. PLGA is a copolymer of PLA and glycolic acid, and its mechanical properties can be adjusted according to the PLA/glycolic acid ratio.[56] By combining their respective characteristics, it provides sufficient strength support to promote cell adhesion.[57] PLGA has been widely used for bone tissue repair due to its excellent biocompatibility, adjustable degradability, and mechanical properties.[58,59] However, PLGA has the disadvantage of weak cell attachment.

2.1.5. PHB. PHB is the most widely studied and commonly used member in biomedical research. PHB is nontoxic and biodegradable, and its degradation products are also biocompatible, some of which are present in natural components of human plasma, such as D-3-hydroxybutyrate.[60] PHB has piezoelectric properties.[61] Due to the surface charge or electrical signal generated by mechanical deformation, PHB is important in stimulating bone growth by regulating cell behavior in piezoelectric polymers.[62] However, compared to other biobased and biodegradable polyesters, it also has some limitations, including a slow degradation rate and high brittleness.[63]

2.1.6. PCS. PCS is a biocompatible and biodegradable synthetic polyester, mainly prepared by polycondensation of citrate and sebacate, with multiple hydroxyl and carboxyl groups in the molecular structure, which makes it easy to cross-link with other molecules or functionalize.[64] PCS has adjustable mechanical properties (adjusted by varying the ratio of citric acid and sebacic acid to change the material's rigidity and flexibility) and good thermal stability. It can be used in BTE and wound dressings, etc. However, due to the disadvantages of its degradation rate, which is difficult to control precisely, and its weak mechanical properties, its application in BTE is limited. Future research can focus on adding nanoparticles, changing the molecular structure, developing copolymers, etc.[65]

2.1.7. PPF. PPF is a biodegradable conjugated polyester, usually prepared by the condensation reaction of fumaric acid and 1,2-propanediol. It has controllable mechanical properties (by adjusting the molecular weight and cross-linking density), biodegradability (by hydrolyzing into small nontoxic molecules with a controllable degradation rate), good biocompatibility, and can be used for BTE.[66] However, PPF has high requirements for cross-linking curing and low thermal stability, and its adaptability to processing conditions needs further optimization.

https://doi.org/10.1021/acsami.4c15719
ACS Appl. Mater. Interfaces XXXX, XXX, XXX−XXX

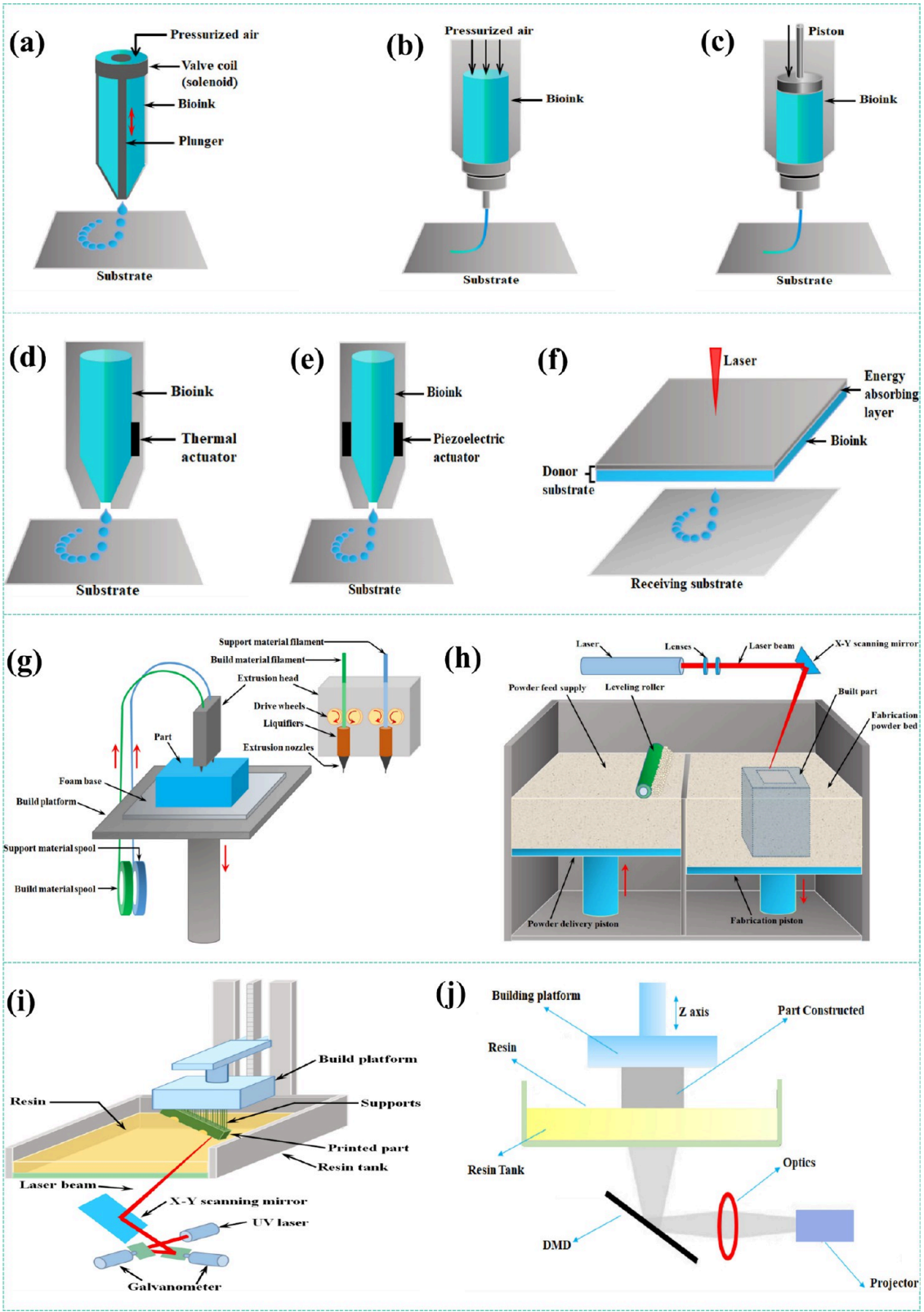

Figure 3. Schematic diagrams of various 3D printing processes. (a) Droplet ejection printing. (b) Pneumatic extrusion printing. (c) Mechanical extrusion printing. (d) Thermal injection printing. (e) Piezoelectric injection printing. (f) Laser-based printing. (g) FDM. (h) SLS. (i) SLA. (j) DLP. Reproduced with permission under a Creative Commons CC-BY 4.0 License from ref 41. Copyright 2024, Prem Ananth, K.; Jayram, N. D.; Elsevier.

2.1.8. PolyActive. PolyActive is a biodegradable multiblock copolymer composed of alternating hydrophilic poly(ethylene glycol) (PEG) and hydrophobic polybutylene terephthalate (PBT) blocks. By adjusting the proportion of components, linear drug release can be achieved, which helps maintain stable drug concentrations. The disadvantage is that the

https://doi.org/10.1021/acsami.4c15719
ACS Appl. Mater. Interfaces XXXX, XXX, XXX−XXX

Table 4. Preparation Methods of Bone Tissue Engineering Scaffolds

3D print type	Method	Advantage	Disadvantage	Ref
Extrusion-based 3D bioprinting	The bioink is extruded through a nozzle and formed into a desired shape on a build platform	On-demand manufacturing, low cost, high structural complexity, high efficiency	Low cell viability, limited print resolution, risk of cross-infection, limitations of print materials	(35)
FDM	Method of melting a thermoplastic polymer into a semiliquid state and extruding the material layer by layer onto a build platform	Low cost and durability, improvement of print processing parameters such as Young's modulus, tensile strength	Low-resolution, the anisotropic, nozzle may be clogged	(36−38)
SLS	Use of laser technology and thermal curing	Highly durable, easily removable support material	Higher cost and printed mats are easily deformed	(39)
MEW	Combines the benefits of electrospinning and 3D printing	No organic solvent, environmental protection, and high efficiency	Higher cost	(40)
SLA	Laser beam scanning and hardening of UV-sensitive materials	High printing precision	The laser has a short service life and a high cost	(41)

Table 5. Comparison of Typical Polyesters[a]

Type	Density/ ($g \cdot cm^{-3}$)	Tensile strength (MPa)	Tensile modulus (GPa)	T_g/°C	T_m/°C	Degradation time (months)	Ref
PLA	1.25−1.27	27.60−50.00	1.00−3.45	50.00−60.00	−	12−16	(46, 47)
PLLA	1.24−1.30	15.50−150.00	2.70−4.14	55.00−65.00	170.00−200.00	>24	(48)
PDLA	1.21−1.25	21.00−60.00	0.35−3.50	45.00−60.00	150.00−162.00	−	(49)
PCL	1.11−1.14	20.70−42.00	0.21−0.44	−60.00−65.00	58.00−65.00	>24	(52, 53)
PGA	1.50−1.71	60.00−99.70	6.00−7.00	35.00−45.00	220.00−233.00	6−12	(56)
PCS	1.15−1.20	0.10−1.96	0.017−6.86	−30.00−30.00	−	1−6	(68)
PPF	0.95−1.20	10.00−50.00	500.00−1000.00	60.00−65.00	−	2−12	(70)
PolyActive	1.10−1.20	1.00−40.00	10.00−500.00	−20.00−50.00	50.00−60.00	>6	(71)
PPC	1.20−1.50	9.00−20.00	50.00−200.00	−20.00−40.00	−	1−6	(72)
PHB	1.54−1.57	17.00−20.00	0.42−0.65	5.00−10.00	173.00−180.00	6−12	(73, 74)
PET	1.35−1.45	50.00−100.00	2500.00−4500.00	67.00−81.00	250.00−260.00	>6	(76)

[a] T_g is the glass transition temperature and T_m is the melting temperature.

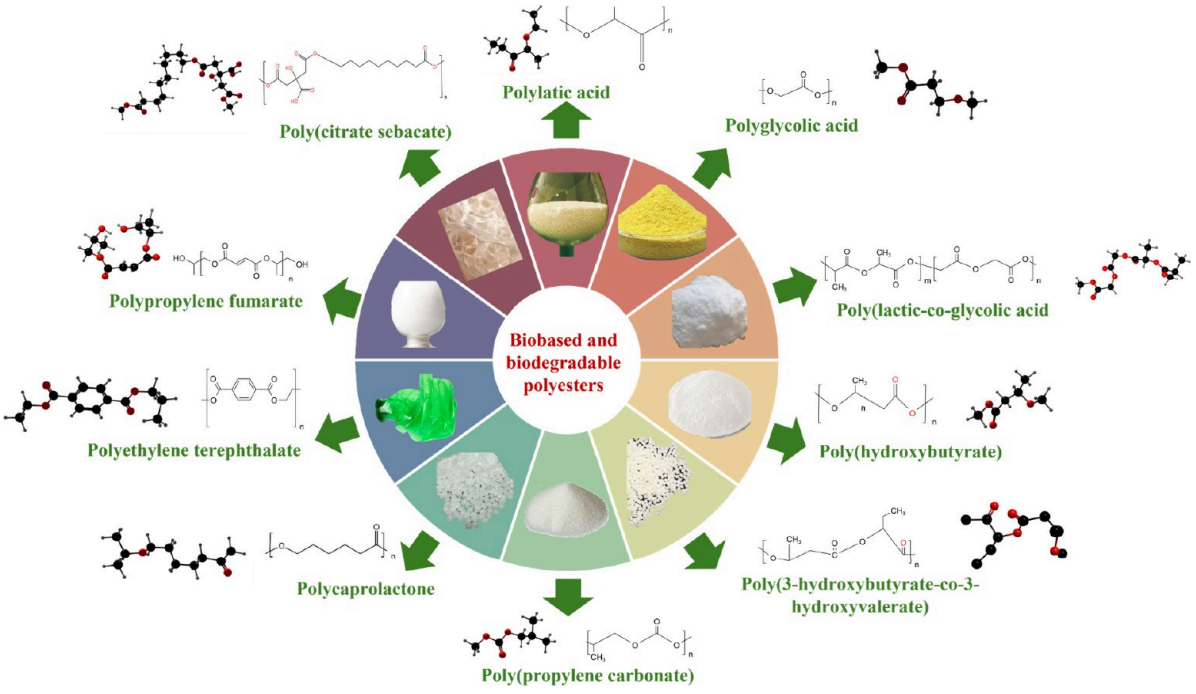

Figure 4. Various biobased and biodegradable polyester structures.

degradation rate of the block copolymer is different, resulting in uneven degradation and low mechanical strength. In addition, the processing conditions require high production costs. Material strength and rigidity can be improved by adding nanoparticles or copolymer design.[67] Surface modification can be carried out to optimize rheological properties, making it more suitable for a 3D printing design.

2.1.9. PPC. PPC is a completely biodegradable and environmentally friendly material made by copolymerizing CO_2 and epichlorohydrin (PO), with the degradation products of CO_2 and water. PPC has the advantages of strong

https://doi.org/10.1021/acsami.4c15719
ACS Appl. Mater. Interfaces XXXX, XXX, XXX−XXX

Table 6. Studies on 3D Printed Biobased and Biodegradable Polyester Scaffolds for BTE

Polyesters	Properties	3D printing technology	Degradation time	Cell types/Animal models	Main findings	Ref
PLA	Pore size: ~ 1000 μm; Porosity: 69.30 ± 7.40%; Compressive modulus: 0.15 ± 0.02 GPa	FDM	Undetected	hFOB cells	Porous spiral scaffolds significantly improved cell spatial separation and promoted cell growth and differentiation.	(80)
PLA/PCL	Pore size:5−15 μm; Porosity: 70.00% ± 4.50%; Compressive modulus: 3.13 ± 1.27 MPa	MEW	Undetected	L929 mouse murine fibroblast and human umbilical vein endothelial (HUVEC) cells	The scaffold presented the highest cell viability value.	(81)
PCL/PLA/PEG	High conversions and low dispersities (<1.5); Compressive modulus: 6.72 GPa	FDM	Undetected	C2C12 murine myoblast cells/Mice subcutaneous implantation	Scaffold promoted osteogenic differentiation *in vitro* and showed good biocompatibility.	(82)
PCL/PLA/PLGA	Compressive modulus: 7.17 MPa	FDM	After 28 days in the culture medium, shape was unrecognizable	Bone marrow derived stem cells (BMSCs), chondrocytes and fat pad derived stem cells (FPSCs)/ Mice subcutaneous implantation and osteochondral defect of goat joint	Scaffolds supported vascularized endochondral bone and phenotypically stable cartilage. After 6 months, hyaline cartilage repair was observed in the animals treated.	(83)
PLLA	Pore size: 450 μm; Porosity: 73%; Compressive modulus: 244 MPa	MEW	Undetected	Human osteoblast-like cells (MG63)	The elastic modulus of the scaffold was equivalent to trabecular bone, and piezoelectric properties was retained. The scaffold had cell compatibility.	(84)
PLLA/PCL/PHBV	Pore size: 800 μm; Porosity: 40%; Compressive modulus: 32 MPa	FDM	Undetected	MC3T3-E1 cells	Alkaline phosphatase activity (ALP) and calcium production in the composite scaffold were significantly higher.	(85)
PLLA/PCL	Pore size: 34.3 ± 12.8 μm; Porosity: 90%; Compressive modulus: 0.22 MPa	FDM	Undetected	HUVECs/A mouse cranial defect model	Scaffolds showed better performance in vascular network formation and new bone formation.	(86)
PCL/PEG	Pore size: 490 ± 25 μm; Porosity: 60%; Compressive modulus: 91 MPa	FDM	Undetected	MC3T3-E1 cells	Scaffolds allowed osteogenic induction and allowed calcium deposition on day 14.	(87)
PGA/PCL	Pore size: 270−540 μm; Porosity: 56 ± 3%; Compressive modulus: 79.7 MPa	FDM	After 10 weeks, the mass degradation loss was 33%.	Mouse fibroblast cells (L-929)	The scaffold had no cytotoxicity and high biocompatibility.	(88)
PPF	Pore size: ~ 500 μm; Porosity: 88.2%; Compressive modulus: 35 MPa	DLP	After 40 days, the mass degradation was about 21%	Undetected	The degree and rate of shape recovery of the compressed scaffold can be controlled and adjusted	(89)
PHB	Pore size: 500−700 μm; Porosity: 55.8 ± 0.7%; Compressive modulus: 0.52 ± 0.01 MPa	SLS	Undetected	rBMSCs	Scaffold promoted controlled release for more than 72 h and had good cell viability and proliferation.	(90)

https://doi.org/10.1021/acsami.4c15719
ACS Appl. Mater. Interfaces XXXX, XXX, XXX−XXX

processing adaptability (can be formed through conventional processing techniques), excellent thermal performance, etc. However, its disadvantages include insufficient mechanical properties (not suitable for high load or high-strength bone scaffold applications), uncontrollable degradation rate (sensitive to environmental factors, unstable degradation), and high industrial costs.[68] In the future, this can be promoted for sustainable development and circular economic applications through structural design and catalyst optimization.

2.1.10. Other Biobased and Biodegradable Polyesters. Poly(3-hydroxybutyrate-*co*-3-hydroxyvalerate) (PHBV) is a polyester with good biodegradability and biocompatibility.[69,70] However, PHBV also has some prominent disadvantages, such as weak mechanical properties, low thermal stability, difficult processing, and high hydrophobicity.[71] Polyethylene terephthalate (PET) is produced by a polycondensation reaction between terephthalic acid (TA) and ethylene glycol (EG), with recurring ester bonds (−COO−) and is one of the representatives of thermoplastic polyesters with excellent mechanical properties, chemical stability, and heat resistance. PET is not a biopolyester material in the strict sense, but there are some specific types that can be categorized as part of the biopolyester, depending on their source and treatment.[72]

2.1.11. Application Prospects of Biobased and Biodegradable Synthetic Polyester in BTE. The development of biobased and biodegradable polyester materials reflects the trend of sustainable and environmentally friendly materials in BTE applications. The development of low-cost biodegradable polymers from renewable resources through green synthesis routes provides promising solutions for biomedical applications.[73] The research on 3D printing a biobased and biodegradable polyester scaffold in BTE is summarized in Table 6. Kolanthai et al.[74] prepared copolyesters based on soybean oil (SO) through melting condensation. The polyester has cell compatibility and may be used as an absorbable biomaterial for BTE and controlled release. Mondal et al.[75,76] showed the potential of SO based materials in manufacturing scaffolds, highlighting the multifunctionality and effectiveness in meeting the complex requirements of BTE. Recycled polyester made from PET waste can be converted into functional materials and applied to BTE, which is a novel chemical recovery strategy for upgrading and recycling.[77] Gomez-Cerezo et al.[72] used 3D printed PET scaffolds to regenerate navicular and lunate bones after fracture. The scaffolds had a high cell viability and enhanced the secretion of fibroblast-associated proteins through mechanical stimulation. Near infrared (NIR) light had a longer wavelength and a greater depth of tissue penetration, so it is widely recommended as a stimulus for BTE applications.[78] NIR was achieved by introducing photoisomerization functional groups into the polymer matrix or by doping suitable photothermal agents into the classical heat-triggered shape memory polymer (SMP) matrix. Choudhury et al.[79] manufactured the NIR response and programmable PLMC scaffold for nanoengineering with polydopamine (PDA) through 3D printing. The scaffold showed a significantly higher osteogenic potential *in vitro*.

However, biobased and biodegradable polyester scaffolds still had some drawbacks in application, such as (1) mechanical strength: as the strength and flexibility of polyester materials may not be sufficient to meet the needs of some special loading environments, especially when used in high stress areas, where they are prone to failure; (2) functional limitations: when functionalized for modification (e.g., incorporation of drugs or biomolecules), the polyester surface activity is low, and additional treatment may be required to improve adhesion efficiency; and (3) higher production costs: certain high-performance polyester materials have more complex synthesis and processing techniques, which may increase manufacturing costs. Therefore, it is imperative to seek new scaffold synthesis strategies to solve this problem.

2.2. Ceramic. Based on the interaction mode and performance with organisms, ceramics used in BTE can be categorized into several categories: (1) biologically inert ceramics, such as alumina and zirconia, are commonly used in dental restoration and bone joint materials; (2) biologically active ceramics, particularly calcium phosphate-based materials (CaPs), include β-TCP, HA, and bioglass (BG); (3) bioceramic composites, such as ceramics combined with other materials (polymers, metals, etc.); (4) functional bioceramics, such as antibacterial ceramics containing elements like silver and copper and piezoelectric ceramics for electric field therapy to promote bone healing. With the development of biomedical technology, the application of ceramics in BTE continues to expand with new materials and technologies emerging regularly.

2.2.1. Alumina. Alumina ceramics (Al_2O_3) are common inorganic ceramic materials with good mechanical properties, chemical stability, and biocompatibility. The Mohs hardness of alumina ceramics is typically around 9, making them suitable for high-wear environment. Alumina ceramics do not cause immune reaction or rejection, making them widely used in medical and dental fields.[91,92] However, it also has some limitations, including low surface smoothness, which may affect the bonding performance with bone tissue. For implants that require close integration with biological tissues, surface treatment or composite materials are necessary to enhance their biological activity.

2.2.2. Zirconia. Compared with alumina ceramics, zirconia ceramics (ZrO_2) have superior toughness and crack resistance, with a blending strength above 900 MPa, which is higher than many common ceramic materials.[93] Zirconia ceramics have significantly better toughness and can remain in the body for extended periods. However, their cost is high and processing is difficult, which limits their application.

2.2.3. CaPs. Calcium phosphate (CaPs), with a chemical composition similar to bone minerals, constitutes a large family of ceramics in BTE.[94,95] When CaP was used as the matrix, a higher sintering temperature is required. This may limit its composite with many materials.[96] Therefore, CaPs are often used as additives for bone layers.

2.2.4. HA. HA ($Ca_{10}(PO_4)_6(OH)_2$) structural components are like those of natural bones and teeth, so they have good biocompatibility. The good biodegradability of HA increases the concentration of Ca^{2+} in the bone defect, thus enhancing the combination between the implant and the bone tissue at the implantation site.[97] In addition, HA also has good bone conductivity, making it a good choice for biobased and biodegradable polyester-based composites. However, its toughness and fatigue resistance are poor.[98]

2.2.5. TCP. TCP has three crystal forms, including α-TCP, β-TCP, and α'-TCP. β-TCP has attracted more and more attention because of its good bioactivity.[99] Although the mechanical strength of HA is higher than that of β-TCP, β-TCP is more absorbable because it has strong bone induction characteristics.[100]

https://doi.org/10.1021/acsami.4c15719
ACS Appl. Mater. Interfaces XXXX, XXX, XXX−XXX

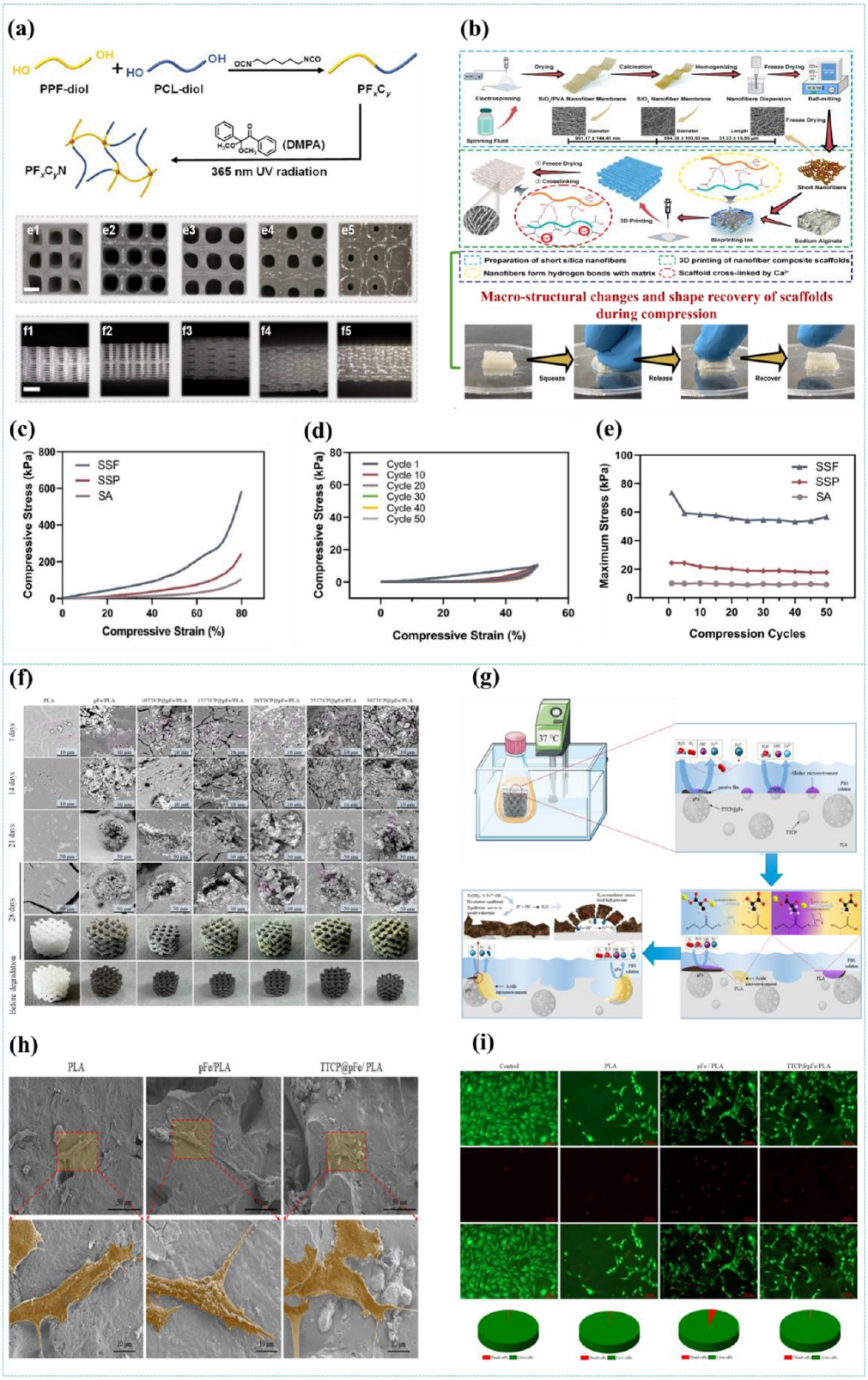

Figure 5. (a) Digital microscopy photographs of PCL/PPF scaffolds photographed from the front and side. Reproduced from ref 110. Copyright 2023, American Chemical Society. (b) Schematic illustration of the fabrication of 3D-printed nanofiber composite scaffolds for bone regeneration. (c) Compressive stress−strain curves. (d) Compressive stress−strain curves of SA scaffolds under 50 cycles in the compressive test at 50% strain. (e) The history of maximum stress with respect to the number of compressive test cycles. Reproduced from ref 116. Copyright 2023, American Chemical Society. (f) Schematic diagram of the 3D printing process and mechanical property testing method. (g) Microscopic and macroscopic morphology of TTCP@pFe/PLA after degradation at different times. (h) Degradation mechanism of TTCP@pFe/PLA scaffold. (i) Adhesion morphology of MC3T3E1 cells after 24 h of culture on scaffolds. Reproduced with permission from ref 122. Copyright 2024, Elsevier.

https://doi.org/10.1021/acsami.4c15719
ACS Appl. Mater. Interfaces XXXX, XXX, XXX−XXX

2.2.6. OCP. Octacalcium phosphate (OCP) is important in biomineralization and bone remodeling.[101] OCP has greater osteoconductivity and biodegradability than those of other calcium phosphate materials. It can cooperate with osteoblasts and osteoclasts through similar coupled metabolic mechanisms.[102] Ca^{2+} and PO_4^{3-} released by OCP in the process of converting into HA provide the ion environment for osteoblasts to mineralize.[103] Due to its excellent osteoinductive and bioactive properties, OCP has the potential to be used in BTE.

2.2.7. BG. BG is a bone tissue substitute with a similar chemical composition and good biocompatibility. BG generally consists of calcium-containing silicates. The most successful commercial brand is 45 S5. The bone-binding mechanism of BG can be attributed to a series of interface reactions that form a bone-like apatite layer on the material surface, while the osteogenic potential of BG is attributed to the released Ca^{2+}, PO_4^{3-}, and Si^{4+} plasmas.[104] Among common ceramic, BG has strong mechanical properties, good biocompatibility and biodegradability, but its degradation speed is slow, and its brittleness is high, so it needs to be compounded with other materials.[105,106]

3. PERFORMANCE REQUIREMENTS OF 3D PRINTED BIOBASED AND BIODEGRADABLE POLYESTER/CERAMIC SCAFFOLD IN BTE

Bone implants for bone repair engineering have been developed from load-bearing pieces with the main goal of load bearing to tissue engineering scaffolds with greater versatility. The design of 3D printed biobased and biodegradable polyester/ceramic scaffolds needs to meet the required mechanical properties and also aims to improve its degradability and biological functionality. The bone repair ability of scaffolds is comprehensively affected by such factors as their micromorphology, macrostructure, mechanical properties, and degradation properties.

3.1. Morphological Structure Parameters. Although 3D printing technology makes the scaffold structure controllable, the design of the internal structure still needs to be deeply explored. Macro-morphology and micro-morphology directly affect the mechanical properties and biological functionality.[107] The macro-morphology of the scaffold refers to the structural parts that can be visually observed, such as the overall structural design, pore size, porosity, and morphology. The micro-morphology refers to its surface roughness and surface element distribution.

The porosity determines the pore size and density of the micropores per unit volume. Higher porosity can promote the exchange of nutrients in body fluids to accelerate cell growth, but increasing the hollow area will also lead to a reduction of the mechanical properties.[108] In order to simulate the extracellular matrix (ECM), the pore size of scaffolds should be within 100−300 μm, within which the nutrient components in body fluid can be transported smoothly.[109] The 3D printed scaffold can have the pore morphology designed, which can guarantee the printing of the precise structure of the scaffold and endow it with additional mechanical properties and biological functionality (Figure 5a).[110] Micromorphology is also an important structural parameter that determines the properties of the scaffold.[111] Biobased and biodegradable polyester/ceramic can print out the designed scaffold structure accurately with high precision due to its good processability.[112] In addition, the use of ceramic as a filler enables the scaffold to have a higher rough surface, so that the scaffold designed with the biobased and biodegradable polyester/ceramic composite material as a matrix has a wider application prospect.

3.2. Mechanical Properties. The basic requirements of scaffolds are that they have similar mechanical properties to the bones implanted in the affected part and can provide sufficient bearing capacity in the early stage of bone repair without causing stress shielding due to excessive strength. In general, the scaffolds in the human body bear compressive stress, and the compressive modulus should be between trabecular bone (0.01−2.0 GPa) and cortical bone (18−25 GPa).[113] The properties of the scaffold can be adjusted within this range, according to the compressive strength required for different implantation sites of bone injury. During implantation, the scaffold is also subjected to other forms of deformation, so tensile, flexural, and torsional properties must also be considered.[114,115] Previous studies have shown that improving the interface compatibility between biobased and biodegradable polyester and ceramic or adding additives[116] (Figure 5b−e) or adjusting the scaffold structure can effectively improve the mechanical properties.[117,118]

3.3. Degradation Properties. Early studies have shown that pure polyester implants have such problems as slow degradation, incomplete degradation, or easy initiation of inflammatory reaction when degraded.[119] The introduction of bioactive ceramic into polyester materials can significantly improve their degradation properties.[120] Daskalakis et al.[121] used PCL as polyester substrate and compounded it with ceramic to prepare scaffolds. The degradation rates of PCL compounded with different ceramic scaffolds were significantly different. The pore size and shape of the scaffold also significantly affect its degradation rate. Adjusting the degradation properties of the scaffold to match its degradation process with the rate of new bone formation in the 3D printing process is also one of the directions of the current research. Ding et al.[122] prepared PLA composite tetracalcium phosphate (TTCP) and porous iron (pFe) scaffolds by SLS (TTCP@pFe/PLA). The alkaline environment generated by the dissolution of TTCP can effectively catalyze the hydrolysis of PLA and accelerate its degradation (Figure 5f,g).

3.4. Biological Function. After the structure, mechanical properties, and degradation rate of the scaffold have met the requirements of bone repair, how to improve the biological functionality of the scaffold becomes particularly critical.[123,124] The biobased and biodegradable polyester/ceramic scaffolds with good cell compatibility, osteogenic activity, bone mineralization capability, antibacterial property, and antitumor property differ from traditional biodegradable bone repair materials, showing multifunctional properties, high specific surface area, and high biological activity.

3.4.1. Cell Compatibility. Good cell compatibility is the basis for the biological functionality of scaffolds. The cell compatibility of the scaffold can be characterized by physical methods (such as determination of surface roughness and hydrophilicity) or biological methods (determination of cell viability, passage speed, etc.).[125] The enhanced hydrophilicity (surface wettability) of biopolyester/ceramic scaffolds provides a favorable environment for improving cellular responses.[126]

3.4.2. Osteogenic Activity. Osteogenic activity refers to the capability of the scaffold to guide the differentiation of osteoblasts to promote bone repair. Osteogenic activity includes osteoconduction, osteoinduction, and osteomineralization.[127] Ding et al.[122] prepared the composite scaffold. The

https://doi.org/10.1021/acsami.4c15719
ACS Appl. Mater. Interfaces XXXX, XXX, XXX−XXX

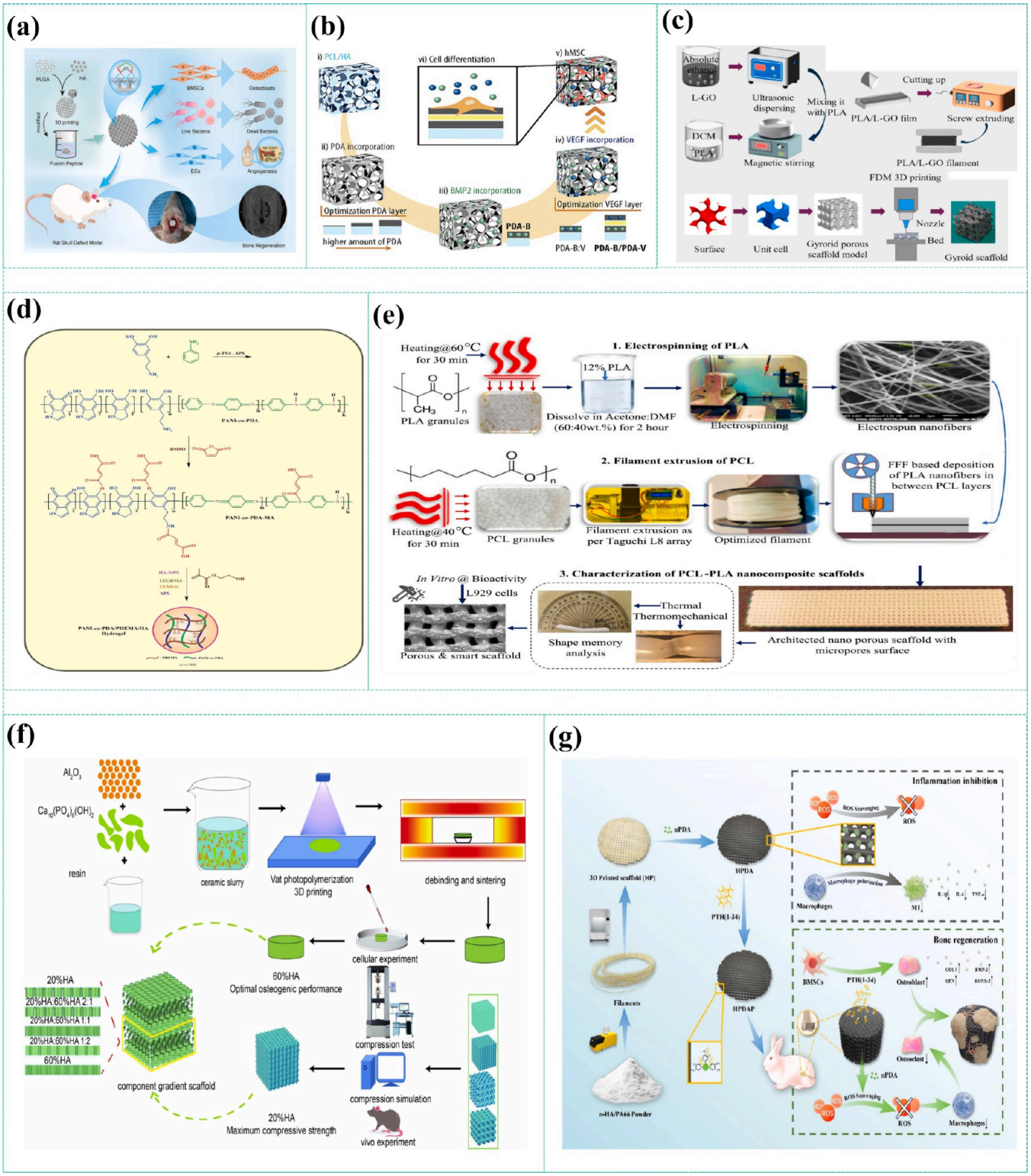

Figure 6. (a) Schematic diagram illustrating the preparation of 3D printed PLGA/HA composite scaffolds modified with fusion peptides. Reproduced with permission under a Creative Comments CC BY-NC-ND 4.0 License from ref 136. Copyright 2024, Liu, Z.; Tian, G.; Liu, L.; Li, Y.; Xu, S.; Du, Y.; Li, M.; Jing, W.; Wei, P.; Zhao, B.; Ma, S.; Deng, J., Elsevier. (b) PCL/HA based composite scaffolds have been fabricated and coated by PDA layer. Reproduced with permission from ref 137. Copyright 2022, Elsevier. (c) Schematic diagram illustrating the preparation of PLA/L-GO composites and bone scaffolds. Reproduced with permission from ref 142. Copyright 2024, Elsevier. (d) Schematic diagram illustrating the preparation PANI/PDA/PHEMA/HA composite scaffolds. Reproduced with permission from ref 146. Copyright 2024, Elsevier. (e) Steps for smart nanoporous scaffolds based on PCL−PLA nanofibers. Reproduced with permission from ref 149. Copyright 2024, Elsevier. (f) Illustration of the preparation of gradient composites and bone scaffolds. Reproduced with permission from ref 157. Copyright 2024, Elsevier. (g) 3D printed porous n-HA/PA66 composite scaffolds. Reproduced with permission from ref 165. Copyright 2024, Elsevier.

https://doi.org/10.1021/acsami.4c15719
ACS Appl. Mater. Interfaces XXXX, XXX, XXX−XXX

dissolution of TTCP formed a localized calcium-rich microenvironment, rapidly inducing the formation of apatite and endowing the scaffold with biological activity. The scaffold exhibited good cell compatibility (Figure 5h,i). Bone conductivity refers to the ability of bioactive factors attached to scaffolds to promote the growth of new bone, and ceramics have excellent bone conductivity.[128] Osteoinduction refers to the process in which bioactive factors promote the differentiation of a tissue or its extract into bone.[129] Increasing the proportion of ceramics in the composite matrix can enhance the osteogenic activity of the scaffold.

3.4.3. Other Properties. The application scenarios of BTE scaffolds are complex; therefore, it is necessary to have other functions required in specific application scenarios. For example, for neoplastic bone defects, tissue-engineered scaffolds need to have certain antitumor properties. Bone tumors cause immense pain to patients and lead to high disability and mortality rates. In the treatment of bone tumors, implanted scaffolds have the potential to eliminate residual tumor cells and avoid tumor recurrence.[130] For the easily infected deep trauma site, the scaffold needs good antibacterial properties.[131] The porous structure mediates water retention properties and ensures good nutrient transport.[132]

4. STRATEGIES FOR IMPROVING THE PROPERTIES OF BIOBASED AND BIODEGRADABLE POLYESTER/CERAMIC SCAFFOLDS

In recent years, to further broaden the application of 3D printed biobased and biodegradable polyester/ceramic scaffolds in the BTE field, researchers have proposed various strategies to improve the structure and performance: (1) regulate the structure, mechanical properties, and degradation rate of the scaffold based on different implantation environments; (2) enhance the ability of scaffolds to promote bone repair, improve cell compatibility, osteogenic activity, bone mineralization, etc.;[133] (3) enhancing the antibacterial and antitumor properties of the scaffold to endow the scaffold with the function of responding to different environments with bone damage.[134] The strategies adopted by domestic and foreign researchers to improve the properties of biobased and biodegradable polyester/ceramic scaffolds in recent years are summarized below.

4.1. Basic Properties. *4.1.1. Mechanical Properties.* When the proportion of ceramic added to the composites is relatively high (20%−50%), it can effectively improve the bioactivity of the composites but also reduce the mechanical properties of the composites.[135] Many bioactive ceramics are introduced into a polyester matrix, easily leading to agglomeration, which reduces the uniformity, resulting in a decrease in the toughness of the material. To improve the compatibility between ceramic and polyester, some scholars added biocompatible interface modifiers, such as new fusion peptides[136] (Figure 6a), PDA[137] (Figure 6b), silane coupling agents, and stearic acid (SA), to reduce the agglomeration of ceramic and enhance the mechanical properties of the scaffold.

Coupling agents can improve the mechanical properties of the scaffold by improving the stress transfer efficiency between the biopolyester and ceramic. Due to the presence of hydrophilic organic functional groups that react with polyester molecules and special functional groups that adsorb onto ceramic surfaces to form strong bonds, coupling agents are used to construct "molecular bridges" at the interface between biopolyesters and ceramics.[138] Jeon et al.[139] fabricated silane-modified raised PCL scaffolds. In mechanical tests, the composite scaffolds exhibited higher mechanical properties (Young's modulus was 1.4 times higher than that of the PCL scaffold). Andrade et al.[140] prepared PLA/SA-coated HA scaffolds by FDM. The SA-coated PLA/HA scaffolds had mechanical properties required for BTE applications. Cheng et al.[141] used citric acid and SA to modify the HA, respectively, and prepared the modified HA/PLA composite scaffold by FDM. The citric acid modified HA composite PLA scaffold had a good compressive modulus.

Adding graphene oxide (GO) and carbon nanotube (CNT) reinforcing agents into a polyester matrix can effectively improve the mechanical properties of composite scaffolds. Ye et al.[142] prepared PLA/L-lysine modified GO scaffolds with triple periodic minimal surface (TPMS) structure using FDM. The scaffold exhibited the highest compressive strength (13.2 MPa) and elastic modulus (226.8 MPa) (Figure 6c). Lan et al.[143] prepared CNT/PLA/HA scaffolds with different CNT additions (0.5−2.0 wt %) using the TIPS method. The results showed that the 1.5 wt % CNT content exhibited the best mechanical properties, with the highest flexural modulus of elasticity (868.5 ± 12.34 MPa), a tensile modulus of elasticity of 209.51 ± 12.73 MPa, and a tensile strength of 3.26 ± 0.61 MPa. PCL is another thermoplastic polyester material with good biodegradability and mechanical flexibility for BTE. Wang et al.[144] used the FDM method to add GO to PCL/HA composite scaffold. GO nanoparticles significantly improved the mechanical properties of PCL.

Appropriate porosity can facilitate cell infiltration and nutrient exchange, promoting bone regeneration. However, higher porosity can affect the mechanical strength of the scaffold, and appropriate mechanical strength is crucial for the structural support of scaffolds at bone defects. Luo et al.[145] composed HA/PLA scaffolds based on selecting appropriate porosity, which effectively balanced the mechanical requirements in the scaffold. Paknia et al.[146] synthesized PDA/polyaniline (PANI) through chemical oxidative polymerization and functionalized it with maleic anhydride (MA), thereby reducing the size to 1.38 μm (Figure 6d). Pérez-Davila et al.[147] prepared PLA/HA composite scaffolds with different PLA/HA ratios and filling percentages by FDM printing. The results showed that within the initial 80 μm (10% of the total pore diameter), HA particles were exponentially distributed, and the scaffold had higher bioavailability and mechanical strength.

The mechanical properties of the scaffold can be adjusted by changing the relative content of biopolyester and ceramics and the geometry. He et al.[148] used fused FDM to fabricate HA and β-TCP reinforced PLA and PCL composites scaffolds. The 10% TCP composite PLA scaffold had the highest compression modulus (152 MPa), which is equivalent to that of human trabecular bone. Kumar et al.[149] prepared a PCL/PLA scaffold, and the acceptable toughness modulus when manufactured using thermal stress relief/preheating (PHT) PCL particles was 7.304 MPa (Figure 6e).

The technical points of 3D printing technology, such as temperature, accuracy, and model design, will further affect the mechanical strength of the scaffold. Premphet et al.[150] studied the effects of nozzle temperature, scaffold density, and printing speed on the mechanical properties of 3D printed PLA/HA composite scaffolds. The mechanical strength of the scaffold can be adjusted by increasing the nozzle temperature and scaffold density, while the printing speed did not affect the compressive strength of the scaffold. Due to the slow

https://doi.org/10.1021/acsami.4c15719
ACS Appl. Mater. Interfaces XXXX, XXX, XXX−XXX

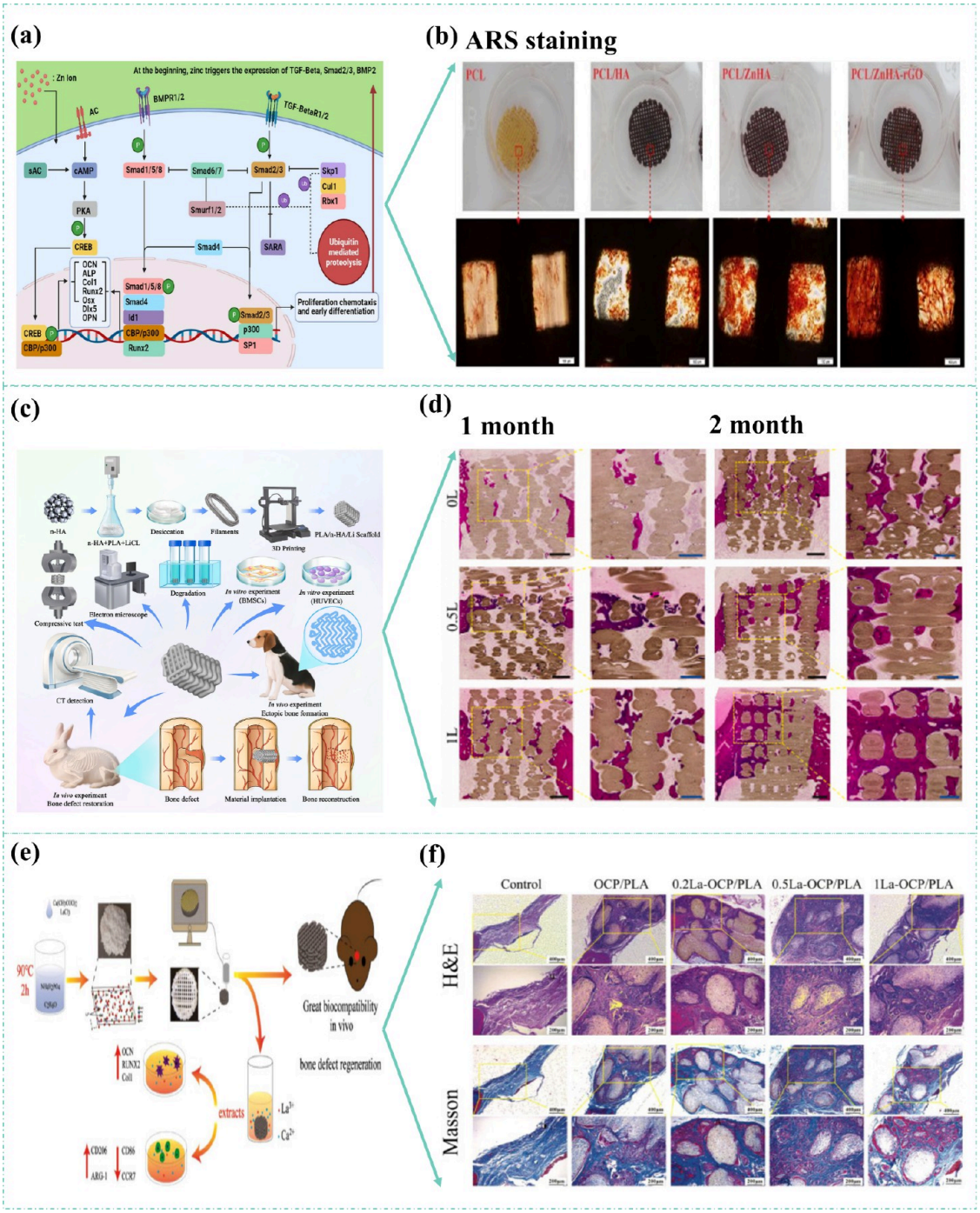

Figure 7. (a) Schematic pathways involved in the osteogenic differentiation of stem cells by Zn ions. (b) ARS staining of PCL and PCL nanocomposite scaffolds after day 14. Reproduced with permission from ref 168. Copyright 2021, Elsevier. (c) Schematic diagram illustrating the preparation and detection of 3D-printed PLA/n-HA/Li composite scaffolds. (d) The scaffolds were implanted into rabbit femurs for 1 and 2 months, followed by H&E staining. Reproduced with permission from ref 169. Copyright 2023, Elsevier. (e) Schematic illustration of the preparation and application of La-OCP/PLA scaffolds. (f) H&E and Masson's trichrome staining of skull specimens implanted with OCP/PLA and La-OCP/PLA scaffolds after 8 weeks. Reproduced with permission from ref 170. Copyright 2022, Elsevier.

crystallization speed of PLA, the crystallinity of PLA can be improved by annealing, thus improving the mechanical properties of the scaffold. After annealing for 30 min, the compressive strength of PLA/HA scaffolds increased from 63.98 to 71.40 MPa. Direct ink writing (DIW), a 3D printing technique capable of printing biologically active substances (e.g., growth factors or drugs) at low temperatures, is an emerging direction in BTE. Li et al.[151] printed and patterned PLA/PCL/n-HA-based scaffolds by DIW technology. The scaffold with a hexagonal pattern had a high mechanical strength and porosity, and the layered pore structure formed in the rolling process had the potential to solve the problem of nozzle blockage and stimulate bone growth and repair.

4.1.2. Degradation Rate. The degradation rate of the BTE scaffold can be adjusted by compounding different biobased and biodegradable polyesters or biomaterials. Therefore, Yan

https://doi.org/10.1021/acsami.4c15719
ACS Appl. Mater. Interfaces XXXX, XXX, XXX−XXX

et al.[152] prepared injectable scaffolds by doping PANI into HA/PLGA. The results showed that the addition of PANI could promote the formation of filamentous fiber byproducts with hydrolysis products, thus accelerating the degradation of the scaffolds. Due to $\pi-\pi$ stacking and hydrogen bonding, the scaffolds with 10 wt % PANI effectively slowed down the decline of the thermal and mechanical properties of the scaffolds during 16 weeks of degradation. Xia et al.[153] introduced PEG into the PCL/nHA scaffolds. It was found that the PEG-added composite scaffolds improved the degradation rate and formed microscopic pores ranging from 20 nm to 4 μm.

4.2. Bone Repair-Promoting Activity. *4.2.1. Cell Compatibility.* Biobased and biodegradable polyester/ceramic scaffolds can be further optimized for promoting bone defect repair performance by combining alginate, graphene, Nano ATP, polyhydroxyalkanoates (PHA), and other materials. Kardan-Halvaei et al.[154] used PLA scaffolds coated with alginate/HA. The scaffold exposed a high cell survival rate of about 97% and had no cytotoxicity. Choudhary et al.[155] coated PLA scaffold with HA using the dip-coating technique. The HA coating made the scaffolds biologically active, exhibiting improved wettability, degradability, and a high cellular response. Kadi et al.[156] prepared nanocomposite scaffolds with different contents of HA/PCL/gelatin. The prepared scaffolds did not negatively affect the viability of MG-63 cells and led to cell proliferation. Nano-ATP is a magnesium−aluminum silicate clay that absorbs substances and is a suitable material for bone repair and regeneration. Liu et al.[157] improved the strength of HA by incorporating Al_2O_3. The HA with 60% had the best biocompatibility (Figure 6f). Dai et al.[158] prepared nano-ATP/PCL scaffolds using 3D printing technology and modified them with NaOH to form a rough surface. HA was prepared on the nano-ATP/PCL scaffolds by using a biomineralization method. The composite scaffolds increased the expression levels of osteogenesis-related genes, which was attributed to the superior ALP activity and calcium deposition ability. PHA has attracted attention as a potential alternative to traditional plastic bone scaffolds due to biocompatibility and biodegradability as well as a variety of favorable properties. Kim et al.[159] prepared PHA scaffolds by FDM printing. The PHA bone scaffolds were then coated with PDA or HA. The PHA−PDA−HA scaffolds showed enhanced cell viability.

To improve the bone integration ability of biopolyester, bioactive materials can be enhanced or deposited on the biopolyester matrix by changing the processing technology. Hariharan et al.[160] used electron beam deposition (EBD) to deposit HA on PCL substrate materials. The HA layer process is an interesting option for enhancing the biocompatibility of additively manufactured scaffolds. The HA-coated PCL substrates demonstrated 22% and 45% increases in cell growth on the encapsulated samples on day 7 and day 15, respectively. Fluorescence microscopy images of cells inoculated on the coated samples clearly showed an enhanced growth of live (green) cells.

4.2.2. Osteogenic Activity. Binding osteoinductive molecules to the surface of biobased and biodegradable polyester/ceramic scaffolds is clinically critical for achieving ideal osseointegration of scaffolds.[161] Bernardo et al.[162] developed a simple bioinspired coating process that was used to improve cell adhesion and osteogenesis of HA/PLGA composite scaffolds. The Arg-Gly-Asp peptide and bone morphogenetic protein (BMP-2) were simultaneously loaded onto the surfaces of HA/PLGA composite substrates. The implantation of peptide-coated HA/PLGA porous scaffolds enhanced *in vivo* osteogenesis for repair of rabbit radial defects. Cucurbitacin B (CuB), a tetracyclic terpene extracted from cucurbitaceae plants, promotes angiogenesis *in vitro*. Cheng et al.[163] used 3D low-temperature rapid prototyping (LT-RP) technology to blend CuB into PLGA/β-TCP scaffold. The results of a rat skull defect model showed that the PLGA/CuB scaffold enhanced angiogenesis and bone regeneration at the bone defect site compared to those of the CuB-free scaffold implant. Salvianolic acid B (SB) has been shown to alleviate the symptoms of osteoporosis by regulating the total metabolic activity and ALP activity of osteoblasts stimulated by glucocorticoid induction. However, SB is unstable in its chemical structure and easily oxidized. Lin et al.[164] incorporated SB into the PLGA/β-TCP scaffold. The SB was stably released from the scaffold. In animal experiments, the effects of SB on new bone formation, mineral deposition rate, and vascular density in scaffolds were enhanced with increasing concentrations of SB. Certain metals or metal ions possess notable osteogenic and restorative properties. However, it is difficult to control their long-term and slow release *in vivo* by conventional introduction, so their combination with BTE scaffolds can effectively improve the overall osteogenic and restorative properties of the scaffolds. Zeng et al.[165] used FDM technology to prepare a 3D printed nano HA/polyamide 66 (n-HA/PA66) composite biological scaffold with a layer of PDA nanoparticles coated with parathyroid hormone (PTH) (1−34) prepared on the surface, which effectively reduced inflammation and enhanced bone integration (Figure 6g).

HA ceramic is widely used as a coating for traditional implant materials such as titanium. This combination continues to be innovated through the addition of one or more other materials (e.g., iron, strontium, cerium, boron nitride, manganese, tannins, wollastonite, simvastatin, etc.).[166] Such ceramic reinforcements improve the mechanical properties, antimicrobial properties, and corrosion resistance (Figure 7). Europium (Eu) is a rare earth metal with the capability of promoting osteogenic differentiation. Sikora et al.[167] showed the cytotoxicity of scaffolds prepared from Nha/PLLA functionalized and doped with Eu (III) ions (10 wt % Eu^{3+}). The biomaterial had no effect on the viability or proliferation rate of human adipose tissue-derived stromal cells (HuASCs). The obtained scaffolds showed bioimaging capabilities. Maleki-Ghaleh et al.[168] incorporated HA, zinc-doped HA, and ZnHA-rGO nanoparticles into a PCL matrix. The cellular osteogenic effect of the PCL scaffolds was enhanced. ZnHA-rGO nanocomposites within the PCL scaffold matrix significantly improved osteogenic differentiation (Figure 7a,b). Wang et al.[169] investigated the combination of PLA, n-HA, and lithium (Li) in 3D printing scaffolds. The scaffold with 1% Li showed optimal osteogenesis and angiogenesis properties *in vitro* and induced heterotopic ligand formation *in vivo* (Figure 7c,d). Lanthanum (La) has great potential in the treatment and prevention of bone diseases, especially osteoporosis and metabolic disorders. However, the sustained and stable release of La^{3+} ions *in vivo* is challenging. Xu et al.[170] prepared La-OCP powder using the coprecipitation method and developed a La-OCP/PLA porous scaffold. At a certain level of La^{3+}, the La-OCP/PLA scaffold extract increased the expression of osteogenic-related genes, thereby promoting the osteogenic differentiation of BMSCs and regulating the immune response

https://doi.org/10.1021/acsami.4c15719
ACS Appl. Mater. Interfaces XXXX, XXX, XXX−XXX

at the fracture site (Figure 7e,f). Mansi et al.[171] utilized metal−organic frameworks (MOFs) to effectively introduce multifunctionality by combining the PCL in MEW with a silver/silver chloride-modified iron-based MOF. The iron component of the MOFs (Fe) made the composite material visible by MRI, which allowed scaffold monitoring at the time of implantation using clinically acceptable methods.

EBM is debris produced by the reaming of bone cavities of the same bone and exhibits significant osteogenic activity because it contains many stem cells.[172] Liu et al.[173] investigated the effect of eBM combined with PLA/HA scaffolds in repairing critical-sized bone defects in a rabbit model. The microcomputed tomography (μCT) analysis at 8 weeks showed that the bone volume (BV) and BV/tissue volume (BV/TV) in the composite scaffold group were significantly higher. Gendviliene et al.[174] investigated PLA/HA scaffold cellularization with ECM. μCT revealed that PLA/HA/ECM produced 1.495 mm^3 more bone volume. Ebrahimi et al.[175] enhanced bone formation, osteogenic differentiation, and *in vitro* biocompatibility by modifying PCL scaffolds with HA and collagen type I (COL I). Sun et al.[176] developed a GO-modified filipin (SF)/nHA scaffold loaded with urogenic stem cells (USCs). Scaffolds with GO content below 0.5% promoted macrophage M2-type differentiation, accelerated bone regeneration, and nearly bridged the cranial defects in rats 12 weeks postoperatively. Chen et al.[177] prepared PCL/HA/simvastatin (PCL/HA/SIM) composites scaffold with a 3D multistage porous structure. The greater HA content promoted the proliferation of mouse embryonic fibroblast (M3T3) cells. Furthermore, incorporating 0.2 wt % SIM into PCL/HA composite scaffolds significantly enhanced proliferation and osteogenic gene expression. Liu et al.[178] prepared a PLA and HA scaffold loaded with eBM combined with induced membrane (IM) to provide growth factors. Coculture with MSCs demonstrated that the scaffold exhibited considerable differentiation potential.

It has been verified by many animal experiments *in vivo* that the biobased and biodegradable polyester/ceramic scaffolds exhibit remarkable osteogenic ability and potential for clinical application. Fazeli et al.[179] conducted a comparative study of PCL scaffolds combined with HA and BG ceramic scaffolds for bone regeneration in cranial defect areas. The results of the study suggested that PCL using HA and BG ceramics had great potential applications in cranial bone defect treatment. Chen et al.[177] developed a 3D scaffold consisting of calreticulin (KGN)-loaded GelMA hydrogel as the upper layer to mimic cartilage-specific ECM and HA-coated 3D-printed PCL/HA as the lower layer to mimic subchondral bone. The bilayer scaffold was subsequently modified with a tannic acid (TA) primer coating and E7 peptide. The scaffold supported cell attachment and proliferation and enhanced the chondrogenic and osteogenic differentiation of BMSCs in specific layers. Zhang et al.[180] prepared vancomycin/PLGA slow-release microspheres (VAN/PLGA-MS). The VAN/PLGA-MS were loaded into the pores of n-HA and PLA scaffolds using dual-nozzle 3D printing at a certain ratio, enabling the composite to promote bone repair and resist local infections. This approach demonstrated the ability to generate vascularized tissue-engineered bone *in vivo*.

4.3. Other Properties. *4.3.1. Antitumor Properties.* Metformin (MET) is an antitumor drug that helps to treat neoplastic bone defects because of its synergistic effect in promoting bone tissue regeneration.[181,182] Harmanci et al.[183] prepared various designs of PCL/PVA, PCL/PVA/PCL, MET loaded PCL/PVA-MET and PCL/PVA-MET/PCL scaffolds. In the study of drug release kinetics, the correlation coefficients (R^2) of PCL/PVA-MET and PCL/PVA-MET/PCL scaffold to the first-order release model were 0.8735 and 0.889, respectively. MET induced the differentiation of mesenchymal stem cells into the osteoblast lineage *in vitro*. Shahrezaee et al.[184] manufactured a PLA/PCL scaffold for delivering MET loaded gelatin nanocarriers to a critical skull defect in a rat model. The expression level of osteogenesis and angiogenesis markers in the composite scaffold increased significantly. The scaffold improved bone ingrowth, angiogenesis, and defect reconstruction. Tan et al.[185] constructed PLLA/nHA/MET nanocomposite scaffolds using SLS technology. The scaffolds had a long drug release time. In addition, the scaffold induced apoptosis in osteosarcoma (OS) cells by upregulating the expression of apoptosis-related genes, exhibited excellent tumor suppression properties *in vitro*, and induced osteogenic differentiation of BMSCs by promoting osteogenic gene expression.

4.3.2. Antibacterial Properties. Open bone defects may be at risk of infection due to deep wounds, difficulty in cleaning, and other issues during the treatment process. Biobased and biodegradable polyester/ceramic scaffolds with certain antibacterial abilities can reduce the probability of concurrent infection during the treatment course and further reduce the risk of treatment for bone defects. Minocycline (MH) is a semisynthetic tetracycline with a broad antibacterial spectrum that also provides anti-inflammation, antioxidation, and antiapoptosis effects by inhibiting bacterial protein synthesis.[186,187] Kakiage et al.[188] performed the functionalized modification of PLA/citric acid-HA (cHA) 3D printing scaffold with COL and MH to reduce the formation of bacterial biofilm. The PLACol-MH and PLA-Col-MH-cHA effectively inhibited the growth of bacteria, with an inhibition zone that was about 26 mm in diameter, while no inhibition zone was observed in the blank MH sample. Li et al.[189] combined the 3D printing technology with the chemical precipitation method to prepare a PLA/PEG/n-HA scaffold doped with dexamethasone (Dex). The cell anti-inflammatory experiment proved that Dex released by the scaffold successfully inhibited the secretion of interleukin-6 and inducible nitric oxide synthase by lipopolysaccharide-induced M1 macrophages and showed good antibacterial properties. Nanosilver (Ag) particles can interact with thiols on bacterial membrane proteins to change the permeability of the membrane and then destroy the integrity of the bacteria, so they have excellent antibacterial properties.[46] Huang et al.[190] introduced nanosilver particles into the PLLA/HA composite material by a solution in situ growth method and then used SLS technology to prepare the scaffold (PLLA@HA@Ag). The results showed that there was no inhibition zone around the PLLA scaffold, while the inhibition zone around the scaffold was significantly larger, indicating that the former had strong antibacterial activity. Turbidity analysis indicated that the turbidity of PLLA scaffold cultures was similar to that of the control group, while the medium incubated with the scaffold group became transparent, indicating that the growth of bacteria in the scaffold group was strongly inhibited. The antibacterial rate of the scaffold was over 92.5%.

4.3.3. Biological Imaging Properties. The bone reconstruction process of the patient can be effectively tracked by utilizing biological imaging function. Eu can emit fluorescence

https://doi.org/10.1021/acsami.4c15719
ACS Appl. Mater. Interfaces XXXX, XXX, XXX−XXX

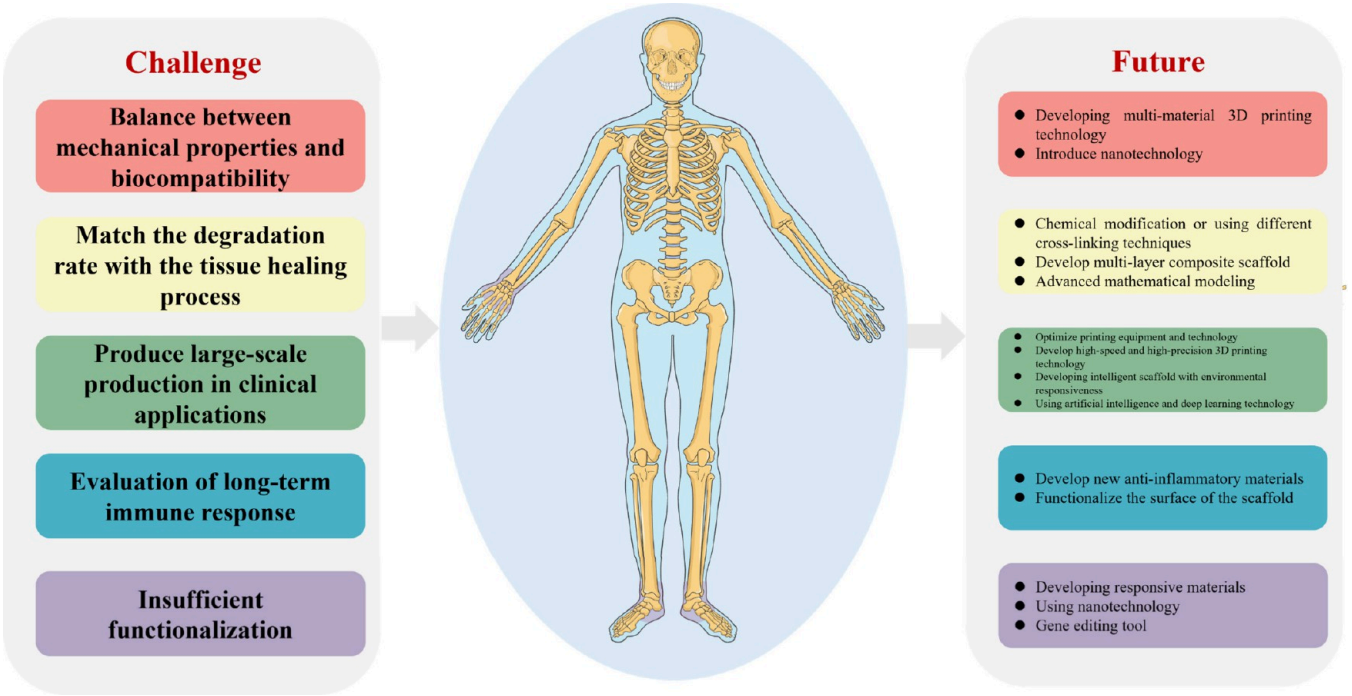

Figure 8. Perspective view and challenges of 3D printed biobased and biodegradable polyester/ceramic composite materials in the BTE field.

under the monitoring of μCT and magnetic resonance imaging technology, which is often applied to biological imaging.[191−194] Marycz et al.[195] used Eu^{3+} modified HA and PLLA to prepare BTE scaffolds. As the HA on the scaffold was converted to new bone, the Eu^{3+} modified on the HA enables the new bone to have fluorescence ability, allowing the regeneration process of bone tissue *in vivo* to be monitored or the passage of cells to be tracked.

5. THE CHALLENGES AND FUTURE PERSPECTIVES OF 3D PRINTED BIOBASED AND BIODEGRADABLE POLYESTER/CERAMIC COMPOSITE MATERIALS IN APPLICATION

3D printed biopolyester/ceramic scaffolds have been widely used in the field of BTE. However, as summarized here, there are still many challenges in practical applications (Figure 8).

5.1. Balance between Mechanical Properties and Biocompatibility. The mechanical properties of composite materials are not enough to meet the needs of some high-load parts. It is difficult to reconcile the flexibility of the biopolyester with the brittleness of the ceramic, which may lead to the decline in the mechanical properties of the scaffold. In the process of 3D printing, problems such as the nozzle and temperature may cause scaffold defects (such as uneven pores) and reduce mechanical stability. In the future, multimaterial 3D printing technology can be developed, and scaffolds with gradient distribution can be prepared by combining the toughness of biopolyester and the rigidity of ceramic to improve mechanical properties and biological function. Nanotechnology can be introduced to optimize the pore structure of scaffolds and enhance cell adhesion and proliferation.

5.2. It Is Difficult to Match the Degradation Rate with the Tissue Healing Process. At present, it is difficult to accurately control the degradation rate of scaffolds, and the process of tissue healing usually requires long-term mechanical support. This mismatch may lead to premature degradation of the scaffold, resulting in incomplete healing, or slow degradation, leading to blocked tissue regeneration. In the future, the molecular structure of biopolyester can be adjusted by chemical modification or by using different cross-linking techniques to adjust the degradation behavior of scaffolds, or multilayer scaffolds can be developed to make different layers have gradient degradation characteristics to meet the organizational needs of different periods. Advanced mathematical modeling can be used to predict the interaction between the scaffold degradation behavior and the healing process, providing theoretical guidance.

5.3. Production at Large Scales in Clinical Applications is Difficult. Small-scale 3D printing technology has difficulty meeting the needs of clinical applications and the high-precision reproduction of complex tissue microstructures (such as vascularization and neural networks). High-performance 3D printing equipment and bioinks are costly. The individual needs of different patients increase the complexity of the manufacturing processes. In the future, printing equipment and technology should be optimized, and high-speed, high-precision 3D printing technology should be developed. Efforts should include the development of an intelligent scaffold with environmental responsiveness to enable dynamic regulation of scaffold performance and accurate release of biological factors and the use of artificial intelligence and deep learning technology to enable personalized customization according to the needs of patients.

5.4. Evaluation of Long-Term Immune Response. In the long term implantation process, the degradation of scaffolds may lead to local pH changes, which cause chronic inflammation. In the future, the long-term effects of scaffold degradation products on the immune system should be further studied. New anti-inflammatory materials should be developed, or immune responses could be relieved by functionalizing the

https://doi.org/10.1021/acsami.4c15719
ACS Appl. Mater. Interfaces XXXX, XXX, XXX−XXX

scaffold surface (such as coating with anti-inflammatory drugs).

5.5. Insufficient Functionalization of Scaffold. At present, the basic supporting function of the scaffold has been widely verified, but its effect of promoting specific tissue functions (such as vascularization or bone regeneration) is limited, and it lacks the ability to efficiently integrate bioactive molecules. In the future, responsive materials can be developed or nanotechnology can be used to improve the load and stability of bioactive factors in scaffolds. Through a new gene editing tool, specific genes can be directly activated at the target site of patients based on the delivery and implantation of scaffolds.

6. CONCLUSION

With the aging of the global population, the application of biobased and biodegradable bone tissue engineering (BTE) scaffolds in bone repair will gradually be promoted. In this study, we focused on the treatment and application of biobased and biodegradable polyester/ceramic scaffolds prepared by 3D printing as well as the challenges and future development prospects. Scaffolds not only have biodegradability and osteogenic activity but also can be flexibly adjusted according to the implantation site and printed accurately, making them a new research hotspot in the field of BTE. However, the application of scaffolds in BTE needs further study. At present, research on scaffolds is still in the stage of *in vitro* trials, and there are few *in vivo* trial cases, which need further improvement. It is imperative to develop new scaffolds to enhance their clinical application. To sum up, by optimizing material design and the manufacturing process and exploring biological mechanisms, the clinical application of scaffolds in BTE will be further promoted, providing a more efficient personalized treatment scheme for patients.

AUTHOR INFORMATION

Corresponding Authors

Hongnan Sun − *Laboratory of Food Chemistry and Nutrition Science, Institute of Food Science and Technology, Chinese Academy of Agricultural Sciences; Key Laboratory of Agro-Products Processing, Ministry of Agriculture and Rural Affairs, Haidian District, Beijing 100193, China;* orcid.org/0000-0003-0631-4775; Phone: +86 10 62815541; Email: sunhongnan@caas.cn; Fax: +86 10 62815541

Taihua Mu − *Laboratory of Food Chemistry and Nutrition Science, Institute of Food Science and Technology, Chinese Academy of Agricultural Sciences; Key Laboratory of Agro-Products Processing, Ministry of Agriculture and Rural Affairs, Haidian District, Beijing 100193, China;* orcid.org/0000-0002-1308-0121; Phone: +86 10 62815541; Email: mutaihua@126.com; Fax: +86 10 62815541

Authors

Shunshun Zhu − *Laboratory of Food Chemistry and Nutrition Science, Institute of Food Science and Technology, Chinese Academy of Agricultural Sciences; Key Laboratory of Agro-Products Processing, Ministry of Agriculture and Rural Affairs, Haidian District, Beijing 100193, China; Laboratory of Biomass and Green Technologies, Gembloux Agro-Bio Tech, University of Liège, 5030 Gembloux, Belgium*

Aurore Richel − *Laboratory of Biomass and Green Technologies, Gembloux Agro-Bio Tech, University of Liège, 5030 Gembloux, Belgium;* orcid.org/0000-0002-4352-6542

Complete contact information is available at: https://pubs.acs.org/10.1021/acsami.4c15719

Notes

The authors declare no competing financial interest.

ACKNOWLEDGMENTS

The authors gratefully acknowledge the earmarked fund for CARS (CARS-10) and the Science and Technology Innovation Project of the Chinese Academy of Agricultural Sciences (CAAS-ASTIP-202X-IFST).

REFERENCES

(1) Deb, P.; Das Lala, S.; Barua, E.; Deoghare, A. B. Physico-Mechanical and Biological Analysis of Composite Bone Scaffold Developed from *Catla Catla* Fish Scale Derived Hydroxyapatite for Bone Tissue Engineering. *Arab. J. Sci. Eng.* **2024**, *49* (1), 27.

(2) Daldiken, E.; Koçak, F. Z.; Küçükdeveci, N. Synthesis and Characterisations of Clinoptilolite Enriched Hydroxyapatite Nano-ceramics by Sol-Gel Route for Bone Regeneration. *Ceram. Int.* **2024**, *50* (11), 19650−19659.

(3) Zhang, L.; Lu, T.; He, F.; Zhang, W.; Yuan, X.; Wang, X.; Ye, J. Physicochemical and Cytological Properties of Poorly Crystalline Calcium-Deficient Hydroxyapatite with Different Ca/P Ratios. *Ceram. Int.* **2022**, *48* (17), 24765−24776.

(4) Zhang, Y.; Jian, Y.; Jiang, X.; Li, X.; Wu, X.; Zhong, J.; Jia, X.; Li, Q.; Wang, X.; Zhao, K.; Yao, Y. Stepwise Degradable PGA-SF Core-Shell Electrospinning Scaffold with Superior Tenacity in Wetting Regime for Promoting Bone Regeneration. *Mater. Today Bio.* **2024**, *26*, 101023.

(5) Sebastiammal, S.; Fathima, A. S. L.; Al-Ghanim, K. A.; Nicoletti, M.; Baskar, G.; Iyyappan, J.; Govindarajan, M. Synthesis and Characterisation of Magnesium-Wrapped Hydroxyapatite Nanomaterials for Biomedical Applications. *Surf. Interfaces* **2024**, *44*, 103779.

(6) Irfa'i, M. A.; Schmahl, W. W.; Pusparizkita, Y. M.; Muryanto, S.; Prihanto, A.; Ismail, R.; Jamari, J.; Bayuseno, A. P. Hydrothermally Synthesized-Nanoscale Carbonated Hydroxyapatite with Calcium Carbonates Derived from Green Mussel Shell Wastes. *J. Mol. Struct.* **2024**, *1306*, 137837.

(7) Peng, S. Y.; Lin, Y. W.; Lin, Y. Y.; Lin, K. L. Hydrothermal Synthesis of Hydroxyapatite Nanocrystals from Calcium-Rich Limestone Sludge Waste: Preparation, Characterization, and Application for Pb^{2+} Adsorption in Aqueous Solution. *Inorg. Chem. Commun.* **2024**, *160*, 111943.

(8) Lee, K.; Kwon, K. Y. Preparation of Amine-Incorporated Hydroxyapatite through a Single-Step Hydrothermal Reaction. *Mater. Lett.* **2024**, *355*, 135508.

(9) Wan, L.; Cui, B.; Wang, L. A Review on Preparation Raw Materials, Synthesis Methods, and Modifications of Hydroxyapatite as Well as Their Environmental Applications. *Sustain. Chem. Pharm.* **2024**, *38*, 101447.

(10) Mirkhalaf, M.; Men, Y.; Wang, R.; No, Y.; Zreiqat, H. Personalized 3D Printed Bone Scaffolds: A Review. *Acta Biomater* **2023**, *156*, 110−124.

(11) Budharaju, H.; Suresh, S.; Sekar, M. P.; De Vega, B.; Sethuraman, S.; Sundaramurthi, D.; Kalaskar, D. M. Ceramic Materials for 3D Printing of Biomimetic Bone Scaffolds - Current State-of-the-Art & Future Perspectives. *Mater. Des.* **2023**, *231*, 112064.

(12) Shuai, C.; Yang, W.; Feng, P.; Peng, S.; Pan, H. Accelerated Degradation of HAP/PLLA Bone Scaffold by PGA Blending Facilitates Bioactivity and Osteoconductivity. *Bioact Mater.* **2021**, *6* (2), 490−502.

(13) Feng, P.; Zhao, R.; Tang, W.; Yang, F.; Tian, H.; Peng, S.; Pan, H.; Shuai, C. Structural and Functional Adaptive Artificial Bone: Materials, Fabrications, and Properties. *Adv. Funct. Mater.* **2023**, *33* (23), 2214726.
(14) Li, J.; Yang, Y.; Sun, Z.; Peng, K.; Liu, K.; Xu, P.; Li, J.; Wei, X.; He, X. Integrated Evaluation of Biomechanical and Biological Properties of the Biomimetic Structural Bone Scaffold: Biomechanics, Simulation Analysis, and Osteogenesis. *Mater. Today Bio.* **2024**, *24*, 100934.
(15) Darghiasi, S. F.; Farazin, A.; Ghazali, H. S. Design of Bone Scaffolds with Calcium Phosphate and Its Derivatives by 3D Printing: A Review. *J. Mech. Behav. Biomed. Mater.* **2024**, *151*, 106391.
(16) Manohar, S. S.; Das, C.; Kakati, V. Bone Tissue Engineering Scaffolds: Materials and Methods. *3D Print. Addit. Manuf.* **2024**, *11* (1), 347−362.
(17) Seehanam, S.; Khrueaduangkham, S.; Sinthuvanich, C.; Sae-Ueng, U.; Srimaneepong, V.; Promoppatum, P. Evaluating the Effect of Pore Size for 3d-Printed Bone Scaffolds. *Heliyon* **2024**, *10* (4), No. e26005.
(18) Shi, Q.; Chen, J.; Chen, J.; Liu, Y.; Wang, H. Application of Additively Manufactured Bone Scaffold: A Systematic Review. *Biofabrication* **2024**, *16* (2), 022007.
(19) Lei, H.; Xiao, W.; Si, W.; Xin, B.; Xin, Z.; Ben, W. Advance in Preparation Methods of Bone Tissue Engineering Scaffolds. *Chin. J. Tissue Eng. Res.* **2024**, *28* (29), 4710−4716.
(20) Shuai, C.; Shi, X.; Yang, F.; Tian, H.; Feng, P. Oxygen Vacancy Boosting Fenton Reaction in Bone Scaffold towards Fighting Bacterial Infection. *Int. J. Extrem. Manuf.* **2024**, *6* (1), 015101.
(21) Meng, D.; Hou, Y.; Kurniawan, D.; Weng, R. J.; Chiang, W. H.; Wang, W. 3D-Printed Graphene and Graphene Quantum Dot-Reinforced Polycaprolactone Scaffolds for Bone-Tissue Engineering. *ACS Appl. Nano Mater.* **2024**, *7* (1), 1245−1256.
(22) Wang, X.; Xie, X.; Chen, Y.; Wang, X.; Xu, X.; Shen, Y.; Mo, X. Electrospun Nanofiber Scaffolds for Soft and Hard Tissue Regeneration. *Chin. J. Tissue Eng. Res.* **2024**, *28* (3), 243−261.
(23) Xu, J.; Huang, H.; Sun, C.; Yu, J.; Wang, M.; Dong, T.; Wang, S.; Chen, X.; Cui, T.; Li, J. Flexible Accelerated-Wound-Healing Antibacterial Hydrogel-Nanofiber Scaffold for Intelligent Wearable Health Monitoring. *ACS Appl. Mater. Interfaces* **2024**, *16* (5), 5438−5450.
(24) Aghaiee, S.; Azdast, T.; Hasanzadeh, R.; Farhangpazhouh, F. Fabrication of Bone Tissue Engineering Scaffolds with a Hierarchical Structure Using Combination of 3D Printing/Gas Foaming Techniques. *J. Appl. Polym. Sci.* **2024**, *141* (16), No. e55238.
(25) Widyastuti, D. A.; Yusuf, Y. The Effect of Power Rate Microwave Heating on Limestone Carbonated Hydroxyapatite Scaffold Using Gas Foaming Method. *Adv. Mat Res.* **2024**, *1179*, 11−18.
(26) Savin, G.; Sastourne-Array, O.; Caillol, S.; Bethry, A.; Assor, M.; David, G.; Nottelet, B. Evaluation of Porous (Poly(Lactide-Co-Glycolide)-Co-(ε-Caprolactone)) Polyurethane for Use in Orthopedic Scaffolds. *Molecules* **2024**, *29* (4), 766.
(27) Xie, X.; Cai, J.; Li, D.; Chen, Y.; Wang, C.; Hou, G.; Steinberg, T.; Rolauffs, B.; EL-Newehy, M.; EL-Hamshary, H.; Jiang, J.; Mo, X.; Zhao, J.; Wu, J. Multiphasic Bone-Ligament-Bone Integrated Scaffold Enhances Ligamentization and Graft-Bone Integration after Anterior Cruciate Ligament Reconstruction. *Bioact Mater.* **2024**, *31*, 178−191.
(28) Ferraro, W.; Civilleri, A.; Gögele, C.; Carbone, C.; Vitrano, I.; Carfi Pavia, F.; Brucato, V.; La Carrubba, V.; Werner, C.; Schäfer-Eckart, K.; Schulze-Tanzil, G. The Phenotype of Mesenchymal Stromal Cell and Articular Chondrocyte Cocultures on Highly Porous Bilayer Poly-L-Lactic Acid Scaffolds Produced by Thermally Induced Phase Separation and Supplemented with Hydroxyapatite. *Polymers* **2024**, *16* (3), 331.
(29) Ko, Y. G.; Smith-Callahan, L. A.; Ma, P. X. Biodegradable Honeycomb-Mimic Scaffolds Consisting of Nanofibrous Walls. *Macromol. Biosci* **2024**, *24* (6), 2300450.
(30) De Luca, A.; Capuana, E.; Carbone, C.; Raimondi, L.; CarfiPavia, F.; Brucato, V.; La Carrubba, V.; Giavaresi, G. Three-Dimensional (3D) Polylactic Acid Gradient Scaffold to Study the Behavior of Osteosarcoma Cells under Dynamic Conditions. *J. Biomed Mater. Res. A* **2024**, *112* (6), 841−851.
(31) Ren, Y.; Zhang, C.; Liu, Y.; Kong, W.; Yang, X.; Niu, H.; Qiang, L.; Yang, H.; Yang, F.; Wang, C.; Wang, J. Advances in 3D Printing of Highly Bioadaptive Bone Tissue Engineering Scaffolds. *ACS Biomater. Sci. Eng.* **2024**, *10* (1), 255−270.
(32) A, L.; Elsen, R.; Nayak, S. Artificial Intelligence-Based 3D Printing Strategies for Bone Scaffold Fabrication and Its Application in Preclinical and Clinical Investigations. *ACS Biomater. Sci. Eng.* **2024**, *10* (2), 677−696.
(33) Matheus, H. R.; Hadad, H.; Guastaldi, F. P. S. The State of 3D Printing of Bioengineered Customized Maxillofacial Bone Scaffolds: A Narrative Review. *Front Oral Maxillofac Med.* **2024**, *6*, 5.
(34) Parvanda, R.; Kala, P.; Sharma, V. Bibliometric Analysis-Based Review of Fused Deposition Modeling 3D Printing Method (1994−2020). *3D Print Addit Manuf* **2024**, *11* (1), 383−405.
(35) Roche, A.; Sanchez-Ballester, N. M.; Bataille, B.; Delannoy, V.; Soulairol, I. Fused Deposition Modelling 3D Printing and Solubility Improvement of BCS II and IV Active Ingredients - A Narrative Review. *J. Controlled Release* **2024**, *365*, 507−520.
(36) Zhang, B.; Teoh, X. Y.; Yan, J.; Gleadall, A.; Belton, P.; Bibb, R.; Qi, S. Development of Combi-Pills Using the Coupling of Semi-Solid Syringe Extrusion 3D Printing with Fused Deposition Modelling. *Int. J. Pharm.* **2022**, *625*, 122140.
(37) Krupova, H.; Sternadelova, K.; Mesicek, J.; Ma, Q. P.; Hajnys, J. Experimental Evaluation of Selectively Laser Sintered Polyamide 12 Surface Treatment for Direct Electrodeposition. *Prog. Org. Coat.* **2024**, *186*, 107968.
(38) Kayalar, C.; Helal, N.; Mohamed, E. M.; Dharani, S.; Khuroo, T.; Kuttolamadom, M. A.; Rahman, Z.; Khan, M. A. In Vitro and In Vivo Testing of 3D-Printed Amorphous Lopinavir Printlets by Selective Laser Sinitering: Improved Bioavailability of a Poorly Soluble Drug. *AAPS PharmSciTech* **2024**, *25*, 20.
(39) Seoane-Viaño, I.; Pérez-Ramos, T.; Liu, J.; Januskaite, P.; Guerra-Baamonde, E.; González-Ramírez, J.; Vázquez-Caruncho, M.; Basit, A. W.; Goyanes, A. Visualizing Disintegration of 3D Printed Tablets in Humans Using MRI and Comparison with in Vitro Data. *J. Controlled Release* **2024**, *365*, 348−357.
(40) Devlin, B. L.; Allenby, M. C.; Ren, J.; Pickering, E.; Klein, T. J.; Paxton, N. C.; Woodruff, M. A. Materials Design Innovations in Optimizing Cellular Behavior on Melt Electrowritten (MEW) Scaffolds. *Adv. Funct Mater.* **2024**, *34* (18), 2313092.
(41) Prem Ananth, K.; Jayram, N. D. A Comprehensive Review of 3D Printing Techniques for Biomaterial-Based Scaffold Fabrication in Bone Tissue Engineering. *Ann. 3D Print Med.* **2024**, *13*, 100141.
(42) Harb, S. V.; Kolanthai, E.; Backes, E. H.; Beatrice, C. A. G.; Pinto, L. A.; Nunes, A. C. C.; Selistre-de-Araújo, H. S.; Costa, L. C.; Seal, S.; Pessan, L. A. Effect of Silicon Dioxide and Magnesium Oxide on the Printability, Degradability, Mechanical Strength and Bioactivity of 3D Printed Poly (Lactic Acid)-Tricalcium Phosphate Composite Scaffolds. *Tissue Eng. Regen Med.* **2024**, *21* (2), 223−242.
(43) Lalnundiki, V.; Rakesh, M.; Saha, P.; Sandhu, H. S.; Dhariwal, J. S. Past, Present and Future Industrial Application of Sugarcane Bagasse: A Literature Review. *AIP Conf Proc.* **2024**, *2962* (1), 020053.
(44) Guo, W.; Bu, W.; Mao, Y.; Wang, E.; Yang, Y.; Liu, C.; Guo, F.; Mai, H.; You, H.; Long, Y. Magnesium Hydroxide as a Versatile Nanofiller for 3D-Printed PLA Bone Scaffolds. *Polymers* **2024**, *16* (2), 198.
(45) Rahatuzzaman, M.; Mahmud, M.; Rahman, S.; Hoque, M. E. Design, Fabrication, and Characterization of 3D-Printed ABS and PLA Scaffolds Potentially for Tissue Engineering. *Results Eng.* **2024**, *21*, 101685.
(46) Shuai, C.; Shi, X.; Wang, K.; Gu, Y.; Yang, F.; Feng, P. Ag-Doped CNT/HAP Nanohybrids in a PLLA Bone Scaffold Show Significant Antibacterial Activity. *Biodes Manuf* **2024**, *7* (2), 105−120.
(47) Krishnan, V. G.; Praveena, N. M.; Raj, R. B. A.; Mohan, K.; Gowd, E. B. Thermoreversible Gels of Poly(l-Lactide)/Poly(d-Lactide) Blends: A Facile Route to Prepare Blend α-Form and

https://doi.org/10.1021/acsami.4c15719
ACS Appl. Mater. Interfaces XXXX, XXX, XXX−XXX

Stereocomplex Aerogels. *ACS Appl. Polym. Mater.* **2023**, *5* (2), 1556−1564.
(48) Štěpánková, K.; Ozaltin, K.; Sáha, P.; Vargun, E.; Domincová-Bergerová, E.; Vesel, A.; Mozetič, M.; Lehocký, M. Carboxymethylated and Sulfated Furcellaran from Furcellaria Lumbricalis and Its Immobilization on PLA Scaffolds. *Polymers* **2024**, *16* (5), 720.
(49) Sakarya, D.; Zorlu, T.; Yücel, S.; Sahin, Y. M.; Özarslan, A. C. Advanced Bioresin Formulation for 3D-Printed Bone Scaffolds: PCLDMA and p-PLA Integration. *Polymers* **2024**, *16* (4), 534.
(50) Afza, S.; Esfahani, H.; Hassanzadeh Chinijani, T.; Sharifi, E. The Role of BSA Protein on the Skin Regeneration Ability of Electrospun PCL/HA Scaffolds, Kinetics of Release and Essential in Vitro Tests. *J. Text Inst* **2024**, *115* (1), 1−13.
(51) Daliri Shadmehri, F.; Karimi, E.; Saburi, E. Electrospun PCL/Fibrin Scaffold as a Bone Implant Improved the Differentiation of Human Adipose-Derived Mesenchymal Stem Cells into Osteo-like Cells. *Int. J. Polym. Mater. Polym. Biomater* **2024**, *73* (1), 71−78.
(52) Hashemi, S. M. J.; Enderami, S. E.; Barzegar, A.; Mansour, R. N. Differentiation of Wharton's Jelly-Derived Mesenchymal Stem Cells into Insulin-Producing Beta Cells with the Enhanced Functional Level on Electrospun PRP-PVP-PCL/PCL Fiber Scaffold. *Tissue Cell* **2024**, *87*, 102318.
(53) Li, X.; Sun, S.; Wang, X.; Dong, W. Polyester Polymer Scaffold-Based Therapeutics for Osteochondral Repair. *J. Drug Deliv Sci. Technol.* **2023**, *90*, 105116.
(54) Feng, P.; Shen, S.; Shuai, Y.; Peng, S.; Shuai, C.; Chen, S. PLLA Grafting Draws GO from PGA Phase to the Interface in PLLA/PGA Bone Scaffold Owing Enhanced Interfacial Interaction. *Sust Mater. Technol.* **2023**, *35*, No. e00566.
(55) Li, J.; Wang, C.; Gao, G.; Yin, X.; Pu, X.; Shi, B.; Liu, Y.; Huang, Z.; Wang, J.; Li, J.; Yin, G. MBG/PGA-PCL Composite Scaffolds Provide Highly Tunable Degradation and Osteogenic Features. *Bioact Mater.* **2022**, *15*, 53−67.
(56) Cheng, Y.; Li, X.; Gu, P.; Mao, R.; Zou, Y.; Tong, L.; Li, Z.; Fan, Y.; Zhang, X.; Liang, J.; Sun, Y. Hierarchical Scaffold with Directional Microchannels Promotes Cell Ingrowth for Bone Regeneration. *Adv. Healthc Mater.* **2024**, *13* (12), No. e2303600.
(57) He, W.; Li, C.; Zhao, S.; Li, Z.; Wu, J.; Li, J.; Zhou, H.; Yang, Y.; Xu, Y.; Xia, H. Integrating Coaxial Electrospinning and 3D Printing Technologies for the Development of Biphasic Porous Scaffolds Enabling Spatiotemporal Control in Tumor Ablation and Osteochondral Regeneration. *Bioact Mater.* **2024**, *34*, 338−353.
(58) Annaji, M.; Mita, N.; Poudel, I.; Boddu, S. H. S.; Fasina, O.; Babu, R. J. Three-Dimensional Printing of Drug-Eluting Implantable PLGA Scaffolds for Bone Regeneration. *Bioengineering* **2024**, *11* (3), 259.
(59) Ke re mu, A.l. m.; Liang, Z. l.; Chen, L.; Tu xun, A. k. b. e.; A bu li ke mu, M. m. t. a. l.; Wu, Y. q. 3D Printed PLGA Scaffold with Nano-Hydroxyapatite Carrying Linezolid for Treatment of Infected Bone Defects. *Biomed Pharmacother* **2024**, *172*, 116228.
(60) Kiany, F.; Sarafraz, N.; Tanideh, N.; Bordbar, H.; Andisheh-Tadbir, A.; Zare, S.; Farshidfar, N.; Zarei, M. Bone Repair Potential of Collagen-Poly(3-Hydroxybutyrate)-Carbon Nanotubes Scaffold Loaded with Mesenchymal Stem Cells for the Reconstruction of Critical-Sized Mandibular Defects. *J. Stomatol Oral Maxillofac Surg* **2024**, *125* (2), 101670.
(61) Toalá, C. U.; Prokhorov, E.; Barcenas, G. L.; Landaverde, M. A. H.; Limón, J. M. Y.; Gervacio-Arciniega, J. J.; Fuentes, O. A.; Tapia, A. M. G. Electrostrictive and Piezoelectrical Properties of Chitosan-Poly(3-Hydroxybutyrate) Blend Films. *Int. J. Biol. Macromol.* **2023**, *250*, 126251.
(62) Strangis, G.; Labardi, M.; Gallone, G.; Milazzo, M.; Capaccioli, S.; Forli, F.; Cinelli, P.; Berrettini, S.; Seggiani, M.; Danti, S.; Parchi, P. 3D Printed Piezoelectric BaTiO3/Polyhydroxybutyrate Nanocomposite Scaffolds for Bone Tissue Engineering. *Bioengineering* **2024**, *11* (2), 193.
(63) Chen, Z.; Song, Y.; Zhang, J.; Liu, W.; Cui, J.; Li, H.; Chen, F. Laminated Electrospun NHA/PHB-Composite Scaffolds Mimicking Bone Extracellular Matrix for Bone Tissue Engineering. *Mater. Sci. Eng., C* **2017**, *72*, 341−351.
(64) Godinho, B.; Nogueira, R.; Gama, N.; Ferreira, A. Synthesis and Characterization of Poly(Glycerol Sebacate), Poly(Glycerol Succinate) and Poly(Glycerol Sebacate-Co-Succinate). *J. Polym. Environ* **2024**, *32* (9), 4330−4347.
(65) Djordjevic, I.; Choudhury, N. R.; Dutta, N. K.; Kumar, S. Poly[Octanediol-Co-(Citric Acid)-Co-(Sebacic Acid)] Elastomers: Novel Bio-Elastomers for Tissue Engineering. *Polym. Int.* **2011**, *60* (3), 333−343.
(66) Cai, Z.; Wan, Y.; Becker, M. L.; Long, Y. Z.; Dean, D. Poly(Propylene Fumarate)-Based Materials: Synthesis, Functionalization, Properties, Device Fabrication and Biomedical Applications. *Biomaterials* **2019**, *208*, 45−71.
(67) Aghajohari, M.; Fazeli-Khosh, H.; Adibi, M.; Sharif, A. Thin Film Composite Membrane Comprising Ionic Liquid/Graphene Oxide in the Selective Layer for Enhanced CO_2 Separation. *ACS Appl. Polym. Mater.* **2024**, *6* (5), 2576−2585.
(68) Gupta, P. K.; Gahtori, R.; Govarthanan, K.; Sharma, V.; Pappuru, S.; Pandit, S.; Mathuriya, A. S.; Dholpuria, S.; Bishi, D. K. Recent Trends in Biodegradable Polyester Nanomaterials for Cancer Therapy. *Mater. Sci. Eng., C* **2021**, *127*, 112198.
(69) Pinho, T. S.; Cibrão, J. R.; Silva, D.; Barata-Antunes, S.; Campos, J.; Afonso, J. L.; Sampaio-Marques, B.; Ribeiro, C.; Macedo, A. S.; Martins, P.; Cunha, C. B.; Lanceros-Mendez, S.; Salgado, A. J. In Vitro Neuronal and Glial Response to Magnetically Stimulated Piezoelectric Poly(Hydroxybutyrate-Co-Hydroxyvalerate) (PHBV)/Cobalt Ferrite (CFO) Microspheres. *Biomater Adv.* **2024**, *159*, 213798.
(70) Taymouri, S.; Hasani, F.; Mirian, M.; Farhang, A.; Varshosaz, J. Biocompatible Nanocomposite Scaffolds Based on Carrageenan Incorporating Hydroxyapatite and Hesperidin Loaded Nanoparticles for Bone Tissue Regeneration. *Polym. Adv. Technol.* **2024**, *35* (1), No. e6284.
(71) Patel, R.; Gómez-Cerezo, M. N.; Huang, H.; Grøndahl, L.; Lu, M. Degradation Behaviour of Porous Poly(Hydroxybutyrate-Co-Hydroxyvalerate) (PHBV) Scaffolds in Cell Culture. *Int. J. Biol. Macromol.* **2024**, *257* (2), 128644.
(72) Gomez-Cerezo, M. N.; Perevoshchikova, N.; Ruan, R.; Moerman, K. M.; Bindra, R.; Lloyd, D. G.; Zheng, M. H.; Saxby, D. J.; Vaquette, C. Additively Manufactured Polyethylene Terephthalate Scaffolds for Scapholunate Interosseous Ligament Reconstruction. *Biomater Adv.* **2023**, *149*, 213397.
(73) Fakhri, V.; Janmaleki Dehchani, A.; Davoudi, S. A.; Tavakoli Dare, M.; Jafari, A.; Nemati Mahand, S.; Dawi, E. A.; Khonakdar, H. A. Advancing Biomedical Frontiers with Functionalized Soybean Oil: Insights into Tissue Engineering and Drug Delivery. *J. Polym. Environ* **2024**, *32*, 5516−5543.
(74) Kolanthai, E.; Sarkar, K.; Meka, S. R. K.; Madras, G.; Chatterjee, K. Copolyesters from Soybean Oil for Use as Resorbable Biomaterials. *ACS Sustain Chem. Eng.* **2015**, *3* (5), 880−891.
(75) Mondal, D.; Willett, T. L. Mechanical Properties of Nanocomposite Biomaterials Improved by Extrusion during Direct Ink Writing. *J. Mech Behav Biomed Mater.* **2020**, *104*, 103653.
(76) Mondal, D.; Srinivasan, A.; Comeau, P.; Toh, Y. C.; Willett, T. L. Acrylated Epoxidized Soybean Oil/Hydroxyapatite-Based Nanocomposite Scaffolds Prepared by Additive Manufacturing for Bone Tissue Engineering. *Mater. Sci. Eng., C* **2021**, *118*, 111400.
(77) Wang, K.; Guo, C.; Li, J.; Wang, K.; Cao, X.; Liang, S.; Wang, J. High Value-Added Conversion and Functional Recycling of Waste Polyethylene Terephthalate (PET) Plastics: A Comprehensive Review. *J. Environ. Chem. Eng.* **2024**, *12*, 113539.
(78) Prakash, A.; Malviya, R.; Sridhar, S. B.; Shareef, J. 4D Printing in Dynamic and Adaptive Bone Implants: Progress in Bone Tissue Engineering. *Bioprinting* **2024**, *44*, No. e00373.
(79) Choudhury, S.; Joshi, A.; Agrawal, A.; Nain, A.; Bagde, A.; Patel, A.; Syed, Z. Q.; Asthana, S.; Chatterjee, K. NIR-Responsive Deployable and Self-Fitting 4D-Printed Bone Tissue Scaffold. *ACS Appl. Mater. Interfaces* **2024**, *16* (37), 49135−49147.

https://doi.org/10.1021/acsami.4c15719
ACS Appl. Mater. Interfaces XXXX, XXX, XXX−XXX

(80) Zhou, X.; Zhou, G.; Junka, R.; Chang, N.; Anwar, A.; Wang, H.; Yu, X. Fabrication of Polylactic Acid (PLA)-Based Porous Scaffold through the Combination of Traditional Bio-Fabrication and 3D Printing Technology for Bone Regeneration. *Colloids Surf. B Biointerfaces* **2021**, *197*, 111420.
(81) Shahverdi, M.; Seifi, S.; Akbari, A.; Mohammadi, K.; Shamloo, A.; Movahhedy, M. R. Melt Electrowriting of PLA, PCL, and Composite PLA/PCL Scaffolds for Tissue Engineering Application. *Sci. Rep* **2022**, *12* (1), 19935.
(82) Teo, Y. C.; Park, E. J.; Guo, J.; Abbas, A.; Smith, R. A. A.; Goh, D.; Yeong, J. P. S.; Cool, S.; Teo, P. Bioactive PCL-Peptide and PLA-Peptide Brush Copolymers for Bone Tissue Engineering. *ACS Appl. Bio Mater.* **2022**, *5* (10), 4770−4778.
(83) Critchley, S.; Sheehy, E. J.; Cunniffe, G.; Diaz-Payno, P.; Carroll, S. F.; Jeon, O.; Alsberg, E.; Brama, P. A. J.; Kelly, D. J. 3D Printing of Fibre-Reinforced Cartilaginous Templates for the Regeneration of Osteochondral Defects. *Acta Biomater* **2020**, *113*, 130−143.
(84) Karanth, D.; Puleo, D.; Dawson, D.; Holliday, L. S.; Sharab, L. Characterization of 3D Printed Biodegradable Piezoelectric Scaffolds for Bone Regeneration. *Clin Exp Dent Res.* **2023**, *9* (2), 398−408.
(85) Kontogianni, G. I.; Bonatti, A. F.; De Maria, C.; Naseem, R.; Melo, P.; Coelho, C.; Vozzi, G.; Dalgarno, K.; Quadros, P.; Vitale-Brovarone, C.; Chatzinikolaidou, M. Promotion of In Vitro Osteogenic Activity by Melt Extrusion-Based PLLA/PCL/PHBV Scaffolds Enriched with Nano-Hydroxyapatite and Strontium Substituted Nano-Hydroxyapatite. *Polymers* **2023**, *15* (4), 1052.
(86) Gu, J.; Zhang, Q.; Geng, M.; Wang, W.; Yang, J.; Khan, A. ur R.; Du, H.; Sha, Z.; Zhou, X.; He, C. Construction of Nanofibrous Scaffolds with Interconnected Perfusable Microchannel Networks for Engineering of Vascularized Bone Tissue. *Bioact Mater.* **2021**, *6* (10), 3254−3268.
(87) Romero-Araya, P.; Cárdenas, V.; Nenen, A.; Martínez, G.; Pavicic, F.; Ehrenfeld, P.; Serandour, G.; Covarrubias, C.; Neira, M.; Moreno-Villoslada, I.; Flores, M. E. Polycaprolactone Scaffolds Prepared by 3D Printing Electrosprayed with Polyethylene Glycol-Polycaprolactone Block Copolymers for Applications in Bone Tissue Engineering. *Polymer* **2023**, *288*, 126448.
(88) Hedayati, S. K.; Behravesh, A. H.; Hasannia, S.; Bagheri Saed, A.; Akhoundi, B. 3D Printed PCL Scaffold Reinforced with Continuous Biodegradable Fiber Yarn: A Study on Mechanical and Cell Viability Properties. *Polymer* **2020**, *83*, 106347.
(89) Le-Fer, G.; Becker, M. 4D Printing of Resorbable Complex Shape-Memory Poly(propylene fumarate) Star Scaffolds. *ACS Appl. Mater. Interfaces* **2020**, *12* (20), 22444−22452.
(90) Saska, S.; Pires, L. C.; Cominotte, M. A.; Mendes, L. S.; Oliveira, M. F.; Maia, I. A.; da Silva, J. V. L.; Ribeiro, S. J. L.; Cirelli, J. A. Three-Dimensional Printing and in Vitro Evaluation of Poly(3-Hydroxybutyrate) Scaffolds Functionalized with Osteogenic Growth Peptide for Tissue Engineering. *Mater. Sci. Eng., C* **2018**, *89*, 265−273.
(91) Varma, M. V.; Kandasubramanian, B.; Ibrahim, S. M. 3D Printed Scaffolds for Biomedical Applications. *Mater. Chem. Phys.* **2020**, *255*, 123642.
(92) Chevalier, J.; Gremillard, L. Ceramics for Medical Applications: A Picture for the next 20 Years. *J. Eur. Ceram Soc.* **2009**, *29* (7), 1245−1255.
(93) Maidin, S.; Loo, H. S.; Alkahari, M. R.; Samat, K. F.; Yahaya, S. H. Bone Scaffold Geometrical Design and Material Selection by Using Analytical Hierarchy Process for Additive Manufacturing Process. *J. Teknol* **2015**, *77* (32), 141−149.
(94) Zarei, M.; Hasanzadeh Azar, M.; Sayedain, S. S.; Shabani Dargah, M.; Alizadeh, R.; Arab, M.; Askarinya, A.; Kaviani, A.; Beheshtizadeh, N.; Azami, M. Material Extrusion Additive Manufacturing of Poly(Lactic Acid)/Ti6Al4V@calcium Phosphate Core-Shell Nanocomposite Scaffolds for Bone Tissue Applications. *Int. J. Biol. Macromol.* **2024**, *255*, 128040.
(95) Li, Z.; Ur Rehman, I.; Shepherd, R.; Douglas, T. E. L. Generation of Pearl/Calcium Phosphate Composite Particles and Their Integration into Porous Chitosan Scaffolds for Bone Regeneration. *J. Funct Biomater* **2024**, *15* (3), 55.
(96) Yu, L.; Cavelier, S.; Hannon, B.; Wei, M. Recent Development in Multizonal Scaffolds for Osteochondral Regeneration. *Bioact. Mater.* **2023**, *25*, 122−159.
(97) Tao, Y.; Jia, M.; Shao-Qiang, Y.; Lai, C. T.; Hong, Q.; Xin, Y.; Hui, J.; Qing-Gang, C.; Jian-Da, X.; Ni-Rong, B. A Novel Fluffy PLGA/HA Composite Scaffold for Bone Defect Repair. *J. Mater. Sci. Mater. Med.* **2024**, *35* (1), 16.
(98) Fan, X.; Zhang, H. Fabrication and Characterization of LaF_3-Reinforced Porous HA/Ti Scaffolds. *Coatings* **2024**, *14* (1), 111.
(99) Han, Y.; Dal-Fabbro, R.; Mahmoud, A. H.; Rahimnejad, M.; Xu, J.; Castilho, M.; Dissanayaka, W. L.; Bottino, M. C. GelMA/TCP Nanocomposite Scaffold for Vital Pulp Therapy. *Acta Biomater* **2024**, *173*, 495−508.
(100) Wang, B.; Ye, X.; Chen, G.; Zhang, Y.; Zeng, Z.; Liu, C.; Tan, Z.; Jie, X. Fabrication and Properties of PLA/β-TCP Scaffolds Using Liquid Crystal Display (LCD) Photocuring 3D Printing for Bone Tissue Engineering. *Front Bioeng Biotechnol* **2024**, *12*, 1273541.
(101) Javkhlan, Z.; Hsu, S. H.; Chen, R. S.; Chen, M. H. 3D-Printed Polycaprolactone Scaffolds Coated with Beta Tricalcium Phosphate for Bone Regeneration. *J. Formos. Med. Assoc.* **2024**, *123* (1), 71−77.
(102) Anu, S.; Siranjeevi, R.; Mohandoss, S.; Kala, K. Stimulation of Bone Ingrowth Using YSZ/ β-TCP/PCL Composite Bilayer Coating on 316 LSS Scaffold for Orthopedic Application. *Chem. Phys. Impact* **2024**, *8*, 100552.
(103) Aoki, K.; Ideta, H.; Komatsu, Y.; Tanaka, A.; Kito, M.; Okamoto, M.; Takahashi, J.; Suzuki, S.; Saito, N. Bone-Regeneration Therapy Using Biodegradable Scaffolds: Calcium Phosphate Bioceramics and Biodegradable Polymers. *Bioengineering* **2024**, *11*, 180.
(104) Li, L.; Lu, P.; Liu, Y.; Yang, J.; Li, S. Three-Dimensional-Bioprinted Bioactive Glass/Cellulose Composite Scaffolds with Porous Structure towards Bone Tissue Engineering. *Polymers* **2023**, *15* (9), 2226.
(105) Manoochehri, H.; Ghorbani, M.; Moosazadeh Moghaddam, M.; Nourani, M. R.; Makvandi, P.; Sharifi, E. Strontium Doped Bioglass Incorporated Hydrogel-Based Scaffold for Amplified Bone Tissue Regeneration. *Sci. Rep* **2022**, *12* (1), 10160.
(106) Han, X.; Zhou, L.; Liu, Z.; Zhang, S.; Wang, Q.; Lu, X.; R I Abueida, M.; Wang, Q.; Zhang, Z.; Zhang, D. Degradation Behavior of Biomedical Partially Degradable Ti-Mg Composite Fabricated by 3D Printing and Pressureless Infiltration. *J. Mater. Res. Technol.* **2024**, *29*, 3192−3204.
(107) Rojas-Rojas, L.; Tozzi, G.; Guillén-Girón, T. A Comprehensive Mechanical Characterization of Subject-Specific 3D Printed Scaffolds Mimicking Trabecular Bone Architecture Biomechanics. *Life* **2023**, *13* (11), 2141.
(108) Zaharin, H. A.; Rani, A. M. A.; Azam, F. I.; Ginta, T. L.; Sallih, N.; Ahmad, A.; Yunus, N. A.; Zulkifli, T. Z. A. Effect of Unit Cell Type and Pore Size on Porosity and Mechanical Behavior of Additively Manufactured Ti6Al4V Scaffolds. *Materials* **2018**, *11* (12), 2402.
(109) Smit, T.; Koppen, S.; Ferguson, S. J.; Helgason, B. Conceptual Design of Compliant Bone Scaffolds by Full-Scale Topology Optimization. *J. Mech Behav Biomed Mater.* **2023**, *143*, 105886.
(110) Du, R.; Zhao, B.; Luo, K.; Wang, M. X.; Yuan, Q.; Yu, L. X.; Yang, K. K.; Wang, Y. Z. Shape Memory Polyester Scaffold Promotes Bone Defect Repair through Enhanced Osteogenic Ability and Mechanical Stability. *ACS Appl. Mater. Interfaces* **2023**, *15* (36), 42930−42941.
(111) Ibrahimi, S.; D'Andrea, L.; Gastaldi, D.; Rivolta, M. W.; Vena, P. Machine Learning Approaches for the Design of Biomechanically Compatible Bone Tissue Engineering Scaffolds. *Comput. Methods Appl. Mech Eng.* **2024**, *423*, 116842.
(112) Gabrieli, R.; Wenger, R.; Mazza, M.; Verné, E.; Baino, F. Design, Stereolithographic 3D Printing, and Characterization of TPMS Scaffolds. *Materials* **2024**, *17* (3), 654.

https://doi.org/10.1021/acsami.4c15719
ACS Appl. Mater. Interfaces XXXX, XXX, XXX−XXX

(113) Celik, D.; Ustundag, C. B. Fabrication of Biomimetic Scaffold through Hybrid Forming Technique. *Int. J. Ceram. Eng. Sci.* **2024**, *6* (3), No. e10210.
(114) Miri, Z.; Haugen, H. J.; Loca, D.; Rossi, F.; Perale, G.; Moghanian, A.; Ma, Q. Review on the Strategies to Improve the Mechanical Strength of Highly Porous Bone Bioceramic Scaffolds. *J. Eur. Ceram. Soc.* **2024**, *44* (1), 23−42.
(115) Kim, T. R.; Kim, M. S.; Goh, T. S.; Lee, J. S.; Kim, Y. H.; Yoon, S. Y.; Lee, C. S. Evaluation of Structural and Mechanical Properties of Porous Artificial Bone Scaffolds Fabricated via Advanced TBA-Based Freeze-Gel Casting Technique. *Appl. Sci.* **2019**, *9* (9), 1965.
(116) Cai, P.; Li, C.; Ding, Y.; Lu, H.; Yu, X.; Cui, J.; Yu, F.; Wang, H.; Wu, J.; EL-Newehy, M.; Abdulhameed, M. M.; Song, L.; Mo, X.; Sun, B. Elastic 3D-Printed Nanofibers Composite Scaffold for Bone Tissue Engineering. *ACS Appl. Mater. Interfaces* **2023**, *15* (47), 54280−54293.
(117) Jahangir Moshayedi, A.; Taheri, M.; Heidari, A.; Abd Alreda, B.; Yuan, Y.; Heidarshenas, B.; Toghraie, D. Fuzzy Modeling and Characterization of Mechanical and Biological Properties of a Selective Laser Melting Shape: A Comprehensive Study. *Opt Laser Technol.* **2024**, *170*, 110171.
(118) Li, Z.; Chen, Z.; Chen, X.; Zhao, R. Design and Evaluation of TPMS-Inspired 3D-Printed Scaffolds for Bone Tissue Engineering: Enabling Tailored Mechanical and Mass Transport Properties. *Compos Struct* **2024**, *327*, 117638.
(119) Tajvar, S.; Hadjizadeh, A.; Samandari, S. S. Scaffold Degradation in Bone Tissue Engineering: An Overview. *Int. Biodeterior. Biodegrad.* **2023**, *180*, 105599.
(120) Feng, P.; Jia, J.; Liu, M.; Peng, S.; Zhao, Z.; Shuai, C. Degradation Mechanisms and Acceleration Strategies of Poly (Lactic Acid) Scaffold for Bone Regeneration. *Mater. Des* **2021**, *210*, 110066.
(121) Daskalakis, E.; Hassan, M. H.; Omar, A. M.; Acar, A. A.; Fallah, A.; Cooper, G.; Weightman, A.; Blunn, G.; Koc, B.; Bartolo, P. Accelerated Degradation of Poly-ε-Caprolactone Composite Scaffolds for Large Bone Defects. *Polymers* **2023**, *15* (3), 670.
(122) Ding, W.; Chen, M.; Du, H.; Guo, X.; Yuan, H.; Li, M.; Xu, Y. Tetracalcium Phosphate/Porous Iron Synergistically Improved the Mechanical, Degradation and Biological Properties of Polylactic Acid Scaffolds. *Int. J. Biol. Macromol.* **2024**, *271*, 132530.
(123) Chocholata, P.; Kulda, V.; Babuska, V. Fabrication of Scaffolds for Bone-Tissue Regeneration. *Materials.* **2019**, *12* (4), 568.
(124) Zhao, C.; Liu, W.; Zhu, M.; Wu, C.; Zhu, Y. Bioceramic-Based Scaffolds with Antibacterial Function for Bone Tissue Engineering: A Review. *Bioact. Mater.* **2022**, *18*, 383−398.
(125) Fang, G.; Rui, S.; Chun, M.; Yi, X. Low-Temperature Condensation Deposition Method for 3D Printing of Bone Tissue Engineering Poly-Llactic Acid/Pearl Powder Composite Scaffold. *Chin. J. Tissue Eng. Res.* **2024**, *28* (17), 2702−2707.
(126) Kumawat, V. S.; Saini, R. K.; Agrawal, A. K.; Khare, D.; Dubey, A. K.; Ghosh, S. B.; Bandyopadhyay-Ghosh, S. Nano-Fluorcanasite-Fluorapatite Reinforced Poly-ε-Caprolactone Based Biomimetic Scaffold: A Synergistic Approach Towards Generation of Conducive Environment for Cell Survival. *J. Polym. Environ* **2024**, *32* (1), 411−429.
(127) Zhang, Y.; Zhai, D.; Xu, M.; Yao, Q.; Zhu, H.; Chang, J.; Wu, C. 3D-Printed Bioceramic Scaffolds with Antibacterial and Osteogenic Activity. *Biofabrication* **2017**, *9* (2), 025037.
(128) Patil, D.; Kumari, S.; Chatterjee, K. Bioinspired Nano-topography on 3D Printed Tissue Scaffold to Impart Mechanobactericidal and Osteogenic Activities. *Colloids Surf. B Biointerfaces* **2023**, *228*, 113401.
(129) Xu, D.; Xu, Z.; Cheng, L.; Gao, X.; Sun, J.; Chen, L. Improvement of the Mechanical Properties and Osteogenic Activity of 3D-Printed Polylactic Acid Porous Scaffolds by Nano-Hydroxyapatite and Nano-Magnesium Oxide. *Heliyon* **2022**, *8* (6), No. e09748.
(130) Huang, Z.; Tian, Z.; Zhu, M.; Wu, C.; Zhu, Y. Recent Advances in Biomaterial Scaffolds for Integrative Tumor Therapy and Bone Regeneration. *Adv. Ther.* **2021**, *4* (3), 212.
(131) Dorazilová, J.; Muchová, J.; Šmerková, K.; Kočiová, S.; Diviš, P.; Kopel, P.; Veselý, R.; Pavliňáková, V.; Adam, V.; Vojtová, L. Synergistic Effect of Chitosan and Selenium Nanoparticles on Biodegradation and Antibacterial Properties of Collagenous Scaffolds Designed for Infected Burn Wounds. *Nanomaterials* **2020**, *10*, 1971.
(132) Xu, Z.; Li, Y.; Xu, D.; Li, L.; Xu, Y.; Chen, L.; Liu, Y.; Sun, J. Improvement of Mechanical and Antibacterial Properties of Porous NHA Scaffolds by Fluorinated Graphene Oxide. *RSC Adv.* **2022**, *12* (39), 25405−25414.
(133) Fendi, F.; Abdullah, B.; Suryani, S.; Usman, A. N.; Tahir, D. Development and Application of Hydroxyapatite-Based Scaffolds for Bone Tissue Regeneration: A Systematic Literature Review. *Bone* **2024**, *183*, 117075.
(134) Song, Z.; Yu, H.; Hou, L.; Dong, Y.; Hu, M.; Wei, P.; Wang, W.; Qian, D.; Cao, S.; Zheng, Z.; Xu, Z.; Zhao, B.; Huang, Y.; Jing, W.; Zhang, X. Mechanics-Resilient HA/SIS-Based Composite Scaffolds with ROS-Scavenging and Bacteria-Resistant Capacity to Address Infected Bone Regeneration. *Adv. Funct Mater.* **2024**, *34*, 2315382.
(135) Zhang, T.; Li, J.; Wang, Y.; Han, W.; Wei, Y.; Hu, Y.; Liang, Z.; Lian, X.; Huang, D. Hydroxyapatite/Polyurethane Scaffolds for Bone Tissue Engineering. *Tissue Eng. Part B Rev.* **2024**, *30* (1), 60−73.
(136) Liu, Z.; Tian, G.; Liu, L.; Li, Y.; Xu, S.; Du, Y.; Li, M.; Jing, W.; Wei, P.; Zhao, B.; Ma, S.; Deng, J. A 3D-Printed PLGA/HA Composite Scaffold Modified with Fusion Peptides to Enhance Its Antibacterial, Osteogenic and Angiogenic Properties in Bone Defect Repair. *J. Mater. Res. Technol.* **2024**, *30*, 5804−5819.
(137) Godoy-Gallardo, M.; Portolés-Gil, N.; López-Periago, A. M.; Domingo, C.; Hosta-Rigau, L. Multi-Layered Polydopamine Coatings for the Immobilization of Growth Factors onto Highly-Interconnected and Bimodal PCL/HA-Based Scaffolds. *Mater. Sci. Eng., C* **2020**, *117*, 111245.
(138) Shuai, C.; Yu, L.; Feng, P.; Gao, C.; Peng, S. Interfacial Reinforcement in Bioceramic/Biopolymer Composite Bone Scaffold: The Role of Coupling Agent. *Colloids Surf. B Biointerfaces* **2020**, *193*, 111083.
(139) Jeon, H. J.; Lee, M.; Yun, S.; Kang, D.; Park, K.; Choi, S.; Choi, E.; Jin, S.; Shim, J. H.; Yun, W. S.; Yoon, B. J.; Park, J. Fabrication and Characterization of 3D-Printed Biocomposite Scaffolds Based on PCL and Silanated Silica Particles for Bone Tissue Regeneration. *Chem. Eng. J.* **2019**, *360*, 519−530.
(140) Cé de Andrade, J.; Cabral, F.; Clemens, F. J.; Leite Vieira, J.; BP Soares, M.; Hotza, D.; Fredel, M. C. Effect of Stearic Acid on the Mechanical and Rheological Properties of PLA/HA Biocomposites. *Mater. Today Commun.* **2023**, *35*, 106357.
(141) Cheng, S.; Chen, L.; Hong, Y.; Song, G.; Liu, H.; Tang, G. Surface Modification of Hydroxyapatite and Its Influences on the Properties of Poly(Lactic Acid)-Based Porous Scaffolds. *Acta Mater. Compos. Sin.* **2018**, *35* (5), 1087−1094.
(142) Ye, X.; Wang, E.; Huang, Y.; Yang, Y.; Zhang, T.; You, H.; Long, Y.; Guo, W.; Liu, B.; Wang, S. Biomolecule-Grafted GO Enhanced the Mechanical and Biological Properties of 3D Printed PLA Scaffolds with TPMS Porous Structure. *J. Mech Behav Biomed Mater.* **2024**, *157*, 106646.
(143) Lan, W.; Wang, M.; Lv, Z.; Li, J.; Chen, F.; Liang, Z.; Huang, D.; Wei, X.; Chen, W. Carbon Nanotubes-Reinforced Polylactic Acid/Hydroxyapatite Porous Scaffolds for Bone Tissue Engineering. *Front Mater. Sci.* **2024**, *18* (1), 240645.
(144) Wang, H.; Domingos, M.; Scenini, F. Advanced Mechanical and Thermal Characterization of 3D Bioextruded Poly(e-Caprolactone)-Based Composites. *Rapid Prototyp J.* **2018**, *24* (4), 731−738.
(145) Luo, Y.; Kim, J. Achieving the Ideal Balance between Biological and Mechanical Requirements in Composite Bone Scaffolds through a Voxel-Based Approach. *Comput. Methods Biomech Biomed Engin* **2024**, 1−14.
(146) Paknia, S.; Izadi, Z.; Moosaipour, M.; Moradi, S.; Khalilzadeh, B.; Jaymand, M.; Samadian, H. Fabrication and Characterization of Electroconductive/Osteoconductive Hydrogel Nanocomposite Based

https://doi.org/10.1021/acsami.4c15719
ACS Appl. Mater. Interfaces XXXX, XXX, XXX−XXX

on Poly(Dopamine-Co-Aniline) Containing Calcium Phosphate Nanoparticles. *J. Mol. Liq.* **2022**, *362*, 119701.
(147) Pérez-Davila, S.; Garrido-Gulías, N.; González-Rodríguez, L.; López-Álvarez, M.; Serra, J.; López-Periago, J. E.; González, P. Physicochemical Properties of 3D-Printed Polylactic Acid/Hydroxyapatite Scaffolds. *Polymers* **2023**, *15* (13), 2849.
(148) He, M.; Zhang, F.; Li, C.; Su, Y.; Qin, Z.; Niu, Y.; Shang, W.; Liu, B. Mechanical Properties and Oral Restoration Applications of 3D Printed Aliphatic Polyester-Calcium Composite Materials. *Alex. Eng. J.* **2024**, *88*, 245−252.
(149) Kumar, R.; Singh, R.; Kumar, V.; Ranjan, N.; Gupta, J.; Bhura, N. On 3D Printed Thermoresponsive PCL-PLA Nanofibers Based Architected Smart Nanoporous Scaffolds for Tissue Reconstruction. *J. Manuf Process* **2024**, *119*, 666−681.
(150) Premphet, P.; Leksakul, K.; Boonyawan, D.; Vichiansan, N. Process Parameters Optimization and Mechanical Properties of 3D PLA/HA Printing Scaffold. *Mater. Today Proc.* **2023**, *72* (4), 1225−1230.
(151) Li, Y.; Chen, L.; Stehle, Y.; Lin, M.; Wang, C.; Zhang, R.; Huang, M.; Li, Y.; Zou, Q. Extrusion-Based 3D-Printed "Rolled-up" Composite Scaffolds with Hierarchical Pore Structure for Bone Growth and Repair. *J. Mater. Sci. Technol.* **2024**, *171*, 222−234.
(152) Yan, H.; Wang, C.; Zhang, Q.; Yu, P.; Xiao, Y.; Wang, C.; Zhang, P.; Hou, G. Conductive Polyaniline Particles Regulating In Vitro Hydrolytic Degradation and Erosion of Hydroxyapatite/Poly(Lactide-Co-Glycolide) Porous Scaffolds for Bone Tissue Engineering. *ACS Biomater Sci. Eng.* **2023**, *9* (3), 1541−1557.
(153) Xia, D.; Hu, Y.; Ma, N.; Zhang, L.; Zheng, Y.; Lin, T.; Qi, J.; Jin, Q. Robust Hierarchical Porous Polycaprolactone/Nano-Hydroxyapatite/Polyethylene Glycol Scaffolds with Boosted in Vitro Osteogenic Ability. *Colloids Surf. A Physicochem Eng. Asp* **2024**, *681*, 132740.
(154) Kardan-Halvaei, M.; Morovvati, M. R.; Angili, S. N.; Saber-Samandari, S.; Razmjooee, K.; Toghraie, D.; Khandan, A. Fabrication of 3D-Printed Hydroxyapatite Using Freeze-Drying Method for Bone Regeneration: RVE and Finite Element Simulation Analysis. *J. Mater. Res. Technol.* **2023**, *24*, 8682−8692.
(155) Choudhary, N.; Ghosh, C.; Sharma, V.; Roy, P.; Kumar, P. Investigations on Effect of Pore Architectures of Additively Manufactured Novel Hydroxyapatite Coated PLA/Al_2O_3 Composite Scaffold for Bone Tissue Engineering. *Rapid Prototyp J.* **2023**, *29* (5), 1061−1079.
(156) Kadi, F.; Dini, G.; Poursamar, S. A.; Ejeian, F. Fabrication and Characterization of 3D-Printed Composite Scaffolds of Coral-Derived Hydroxyapatite Nanoparticles/Polycaprolactone/Gelatin Carrying Doxorubicin for Bone Tissue Engineering. *J. Mater. Sci. Mater. Med.* **2024**, *35* (1), 7.
(157) Liu, Q.; Tang, Q.; Huang, Z.; Li, Z.; Wang, X.; Wen, P.; Bai, Y.; Chen, F. Functionally Graded Triply Periodic Minimal Surface Scaffold of HA-Al_2O_3 via Vat Photopolymerization 3D Printing. *Addit Manuf* **2024**, *84*, 104117.
(158) Dai, T.; Wu, X.; Liu, C.; Ni, S.; Li, J.; Zhang, L.; Wang, J.; Tan, Y.; Fan, S.; Zhao, H. Biomimetic Hydroxyapatite on 3D-Printed Nanoattapulgite/Polycaprolactone Scaffolds for Bone Regeneration of Rat Cranium Defects. *ACS Biomater Sci. Eng.* **2024**, *10* (1), 455−467.
(159) Kim, D.; Lee, S. J.; Lee, D.; Seok, J. M.; Yeo, S. J.; Lim, H.; Lee, J. J.; Song, J. H.; Lee, K.; Park, W. H.; Park, S. A. Biomimetic Mineralization of 3D-Printed Polyhydroxyalkanoate-Based Microbial Scaffolds for Bone Tissue Engineering. *Int. J. Bioprint* **2024**, *10* (2), 1806.
(160) Hariharan, K.; Selvakumar, M.; Ramkumar, T.; Chandramohan, P. Cell Viability and Bioactive Coating on Additive Manufactured Polycaprolactone Substrate for Osteointegration Applications. *Chem. Phys. Impact* **2024**, *8*, 100409.
(161) Anjum, S.; Arya, D. K.; Saeed, M.; Ali, D.; Athar, M. S.; Yulin, W.; Alarifi, S.; Wu, X.; Rajinikanth, P. S.; Ao, Q. Multifunctional Electrospun Nanofibrous Scaffold Enriched with Alendronate and Hydroxyapatite for Balancing Osteogenic and Osteoclast Activity to Promote Bone Regeneration. *Front Bioeng Biotechnol* **2023**, *11*, 1302594.
(162) Bernardo, M. P.; da Silva, B. C. R.; Hamouda, A. E. I.; de Toledo, M. A. S.; Schalla, C.; Rütten, S.; Goetzke, R.; Mattoso, L. H. C.; Zenke, M.; Sechi, A. PLA/Hydroxyapatite Scaffolds Exhibit In vitro Immunological Inertness and Promote Robust Osteogenic Differentiation of Human Mesenchymal Stem Cells without Osteogenic Stimuli. *Sci. Rep* **2022**, *12* (1), 2333.
(163) Cheng, W. X.; Liu, Y. Z.; Meng, X. B.; Zheng, Z. T.; Li, L. L.; Ke, L. Q.; Li, L.; Huang, C. S.; Zhu, G. Y.; Pan, H. D.; Qin, L.; Wang, X. L.; Zhang, P. PLGA/β-TCP Composite Scaffold Incorporating Cucurbitacin B Promotes Bone Regeneration by Inducing Angiogenesis. *J. Orthop Translat* **2021**, *31*, 41−51.
(164) Lin, S.; Cui, L.; Chen, G.; Huang, J.; Yang, Y.; Zou, K.; Lai, Y.; Wang, X.; Zou, L.; Wu, T.; Cheng, J. C. Y.; Li, G.; Wei, B.; Lee, W. Y. W. PLGA/β-TCP Composite Scaffold Incorporating Salvianolic Acid B Promotes Bone Fusion by Angiogenesis and Osteogenesis in a Rat Spinal Fusion Model. *Biomaterials* **2019**, *196*, 109−121.
(165) Zeng, Z.; Wang, L.; Qu, B.; Gui, X.; Zhang, B.; Deng, Z.; Qin, Y.; Li, Z.; Li, Q.; Wang, L.; Fan, Y.; Zhou, C.; Song, Y. Enhanced Osteogenesis and Inflammation Suppression in 3D Printed N-HA/PA66 Composite Scaffolds with PTH(1−34)-Loaded NPDA Coatings. *Compos B Eng.* **2024**, *282*, 111566.
(166) Fendi, F.; Abdullah, B.; Suryani, S.; Raya, I.; Tahir, D.; Iswahyudi, I. Hydroxyapatite Based for Bone Tissue Engineering: Innovation and New Insights in 3D Printing Technology. *Polym. Bull.* **2024**, *81* (2), 1097−1116.
(167) Sikora, M.; Marcinkowska, K.; Marycz, K.; Wiglusz, R. J.; Śmieszek, A. The Potential Selective Cytotoxicity of Poly (L-Lactic Acid)-Based Scaffolds Functionalized with Nanohydroxyapatite and Europium (III) Ions toward Osteosarcoma Cells. *Materials* **2019**, *12* (22), 3779.
(168) Maleki-Ghaleh, H.; Hossein Siadati, M.; Fallah, A.; Zarrabi, A.; Afghah, F.; Koc, B.; Dalir Abdolahinia, E.; Omidi, Y.; Barar, J.; Akbari-Fakhrabadi, A.; Beygi-Khosrowshahi, Y.; Adibkia, K. Effect of Zinc-Doped Hydroxyapatite/Graphene Nanocomposite on the Physicochemical Properties and Osteogenesis Differentiation of 3D-Printed Polycaprolactone Scaffolds for Bone Tissue Engineering. *Chem. Eng. J.* **2021**, *426*, 131321.
(169) Wang, W.; Wei, J.; Lei, D.; Wang, S.; Zhang, B.; Shang, S.; Bai, B.; Zhao, C.; Zhang, W.; Zhou, C.; Zhou, H.; Feng, S. 3D Printing of Lithium Osteogenic Bioactive Composite Scaffold for Enhanced Bone Regeneration. *Compos B Eng.* **2023**, *256*, 110641.
(170) Xu, Z.; Lin, B.; Zhao, C.; Lu, Y.; Huang, T.; Chen, Y.; Li, J.; Wu, R.; Liu, W.; Lin, J. Lanthanum Doped Octacalcium Phosphate/Polylactic Acid Scaffold Fabricated by 3D Printing for Bone Tissue Engineering. *J. Mater. Sci. Technol.* **2022**, *118*, 229−242.
(171) Mansi, S.; Dummert, S. V.; Topping, G. J.; Hussain, M. Z.; Rickert, C.; Mueller, K. M. A.; Kratky, T.; Elsner, M.; Casini, A.; Schilling, F.; Fischer, R. A.; Lieleg, O.; Mela, P. Introducing Metal-Organic Frameworks to Melt Electrowriting: Multifunctional Scaffolds with Controlled Microarchitecture for Tissue Engineering Applications. *Adv. Funct Mater.* **2024**, *34* (2), 2304907.
(172) Yu, X.; Jiang, S.; Li, D.; Shen, S. G.; Wang, X.; Lin, K. Osteoimmunomodulatory Bioinks for 3D Bioprinting Achieve Complete Regeneration of Critical-Sized Bone Defects. *Compos B Eng.* **2024**, *273*, 111256.
(173) Liu, Z.; Chu, W.; Zhang, L.; Wang, Y.; Zhai, Z.; Liu, F. The Effect of Enhanced Bone Marrow in Conjunction with 3D-Printed PLA-HA in the Repair of Critical-Sized Bone Defects in a Rabbit Model. *Ann. Transl Med.* **2021**, *9* (14), 1134.
(174) Gendviliene, I.; Simoliunas, E.; Alksne, M.; Dibart, S.; Jasiuniene, E.; Cicenas, V.; Jacobs, R.; Bukelskiene, V.; Rutkunas, V. Effect of Extracellular Matrix and Dental Pulp Stem Cells on Bone Regeneration with 3D Printed PLA/HA Composite Scaffolds. *Eur. Cell Mater.* **2021**, *41*, 204−215.
(175) Ebrahimi, Z.; Irani, S.; Ardeshirylajimi, A.; Seyedjafari, E. Enhanced Osteogenic Differentiation of Stem Cells by 3D Printed

https://doi.org/10.1021/acsami.4c15719
ACS Appl. Mater. Interfaces XXXX, XXX, XXX−XXX

PCL Scaffolds Coated with Collagen and Hydroxyapatite. *Sci. Rep* **2022**, *12* (1), 12539.
(176) Sun, J.; Li, L.; Xing, F.; Yang, Y.; Gong, M.; Liu, G.; Wu, S.; Luo, R.; Duan, X.; Liu, M.; Zou, M.; Xiang, Z. Graphene Oxide-Modified Silk Fibroin/Nanohydroxyapatite Scaffold Loaded with Urine-Derived Stem Cells for Immunomodulation and Bone Regeneration. *Stem Cell Res. Ther* **2021**, *12* (1), 591.
(177) Chen, X.; Liu, Y.; Liu, H.; Li, L.; Liu, Y.; Liu, P.; Yang, X. Bioactive Bone Scaffolds Manufactured by 3D Printing and Sacrificial Templating of Poly(ε-Caprolactone) Composites as Filler for Bone Tissue Engineering. *J. Mater. Sci.* **2023**, *58* (12), 5444−5455.
(178) Liu, Z.; Ge, Y.; Zhang, L.; Wang, Y.; Guo, C.; Feng, K.; Yang, S.; Zhai, Z.; Chi, Y.; Zhao, J.; Liu, F. The Effect of Induced Membranes Combined with Enhanced Bone Marrow and 3D PLA-HA on Repairing Long Bone Defects in Vivo. *J. Tissue Eng. Regen Med.* **2020**, *14* (10), 1403.
(179) Fazeli, N.; Arefian, E.; Irani, S.; Ardeshirylajimi, A.; Seyedjafari, E. Accelerated Reconstruction of Rat Calvaria Bone Defect Using 3D-Printed Scaffolds Coated with Hydroxyapatite/Bioglass. *Sci. Rep* **2023**, *13* (1), 12145.
(180) Zhang, P.; Chen, J.; Sun, Y.; Cao, Z.; Zhang, Y.; Mo, Q.; Yao, Q.; Zhang, W. A 3D Multifunctional Bi-Layer Scaffold to Regulate Stem Cell Behaviors and Promote Osteochondral Regeneration. *J. Mater. Chem. B* **2023**, *11* (6), 1240−1261.
(181) Chao, Y.; Wei, T.; Li, Q.; Liu, B.; Hao, Y.; Chen, M.; Wu, Y.; Song, F.; Chen, Q.; Liu, Z. Metformin-Containing Hydrogel Scaffold to Augment CAR-T Therapy against Post-Surgical Solid Tumors. *Biomaterials* **2023**, *295*, 122052.
(182) Zhao, Z.; Liu, J.; Schneider, A.; Gao, X.; Ren, K.; Weir, M. D.; Zhang, N.; Zhang, K.; Zhang, L.; Bai, Y.; Xu, H. H. K. Human Periodontal Ligament Stem Cell Seeding on Calcium Phosphate Cement Scaffold Delivering Metformin for Bone Tissue Engineering. *J. Dent* **2019**, *91*, 103220.
(183) Harmanci, S.; Dutta, A.; Cesur, S.; Sahin, A.; Gunduz, O.; Kalaskar, D. M.; Ustundag, C. B. Production of 3D Printed Bi-Layer and Tri-Layer Sandwich Scaffolds with Polycaprolactone and Poly (Vinyl Alcohol)-Metformin towards Diabetic Wound Healing. *Polymers* **2022**, *14* (23), 5306.
(184) Shahrezaee, M.; Salehi, M.; Keshtkari, S.; Oryan, A.; Kamali, A.; Shekarchi, B. In Vitro and in Vivo Investigation of PLA/PCL Scaffold Coated with Metformin-Loaded Gelatin Nanocarriers in Regeneration of Critical-Sized Bone Defects. *Nanomedicine* **2018**, *14* (7), 2061−2073.
(185) Tan, W.; Gao, C.; Feng, P.; Liu, Q.; Liu, C.; Wang, Z.; Deng, Y.; Shuai, C. Dual-Functional Scaffolds of Poly(L-Lactic Acid)/Nanohydroxyapatite Encapsulated with Metformin: Simultaneous Enhancement of Bone Repair and Bone Tumor Inhibition. *Mater. Sci. Eng., C* **2021**, *120*, 111592.
(186) Zegre, M.; Barros, J.; Ribeiro, I. A. C.; Santos, C.; Caetano, L. A.; Gonçalves, L.; Monteiro, F. J.; Ferraz, M. P.; Bettencourt, A. Poly(DL-Lactic Acid) Scaffolds as a Bone Targeting Platform for the Co-Delivery of Antimicrobial Agents against S. Aureus-C.Albicans Mixed Biofilms. *Int. J. Pharm.* **2022**, *622*, 121832.
(187) Fan, S.; Talha, M.; Yu, X.; Lei, H.; Tan, Y.; Zhang, H.; Lin, Y.; Zhou, C.; Fan, Y. 3D Printing of Porous Ti6Al4V Bone Tissue Engineering Scaffold and Surface Anodization Preparation of Nanotubes to Enhance Its Biological Property. *Nanotechnol Rev.* **2023**, *12* (1), 572.
(188) Kakiage, M.; Iwase, K.; Kobayashi, H. Effect of Citric Acid Addition on Disaggregation of Crystalline Hydroxyapatite Nanoparticles under Calcium-Rich Conditions. *Mater. Lett.* **2015**, *156*, 39−41.
(189) Li, X.; Wang, Y.; Wang, Z.; Qi, Y.; Li, L.; Zhang, P.; Chen, X.; Huang, Y. Composite PLA/PEG/NHA/Dexamethasone Scaffold Prepared by 3D Printing for Bone Regeneration. *Macromol. Biosci* **2018**, *18* (6), 1800068.
(190) Huang, J.; Cheng, C.; Yang, Y.; Zan, J.; Shuai, C. Zeolitic Imidazolate Frameworks Serve as an Interface Layer for Designing Bifunctional Bone Scaffolds with Antibacterial and Osteogenic Performance. *Nanomaterials* **2023**, *13* (21), 2828.
(191) Leyhausen, J.; Schäfer, T.; Gurr, C.; Berg, L. M.; Seelemeyer, H.; Pretzsch, C. M.; Loth, E.; Oakley, B.; Buitelaar, J. K.; Beckmann, C. F.; Floris, D. L.; Charman, T.; Bourgeron, T.; Banaschewski, T.; Jones, E. J. H.; Tillmann, J.; Chatham, C.; Ahmad, J.; Ambrosino, S.; Auyeung, B.; Baron-Cohen, S.; Baumeister, S.; Bölte, S.; Bours, C.; Brammer, M.; Brandeis, D.; Brogna, C.; de Bruijn, Y.; Chakrabarti, B.; Cornelissen, I.; Crawley, D.; Dell'Acqua, F.; Dumas, G.; Durston, S.; Ecker, C.; Faulkner, J.; Frouin, V.; Garcés, P.; Goyard, D.; Ham, L.; Hayward, H.; Hipp, J.; Holt, R.; Johnson, M. H.; Kundu, P.; Lai, M. C.; D'ardhuy, X. L.; Lombardo, M. V.; Lythgoe, D. J.; Mandl, R.; Marquand, A.; Mason, L.; Mennes, M.; Meyer-Lindenberg, A.; Moessnang, C.; Bast, N.; O'Dwyer, L.; Oldehinkel, M.; Oranje, B.; Pandina, G.; Persico, A. M.; Ruggeri, B.; Ruigrok, A.; Sabet, J.; Sacco, R.; San JoséCáceres, A.; Simonoff, E.; Spooren, W.; Toro, R.; Tost, H.; Waldman, J.; Williams, S. C. R.; Wooldridge, C.; Zwiers, M. P.; Murphy, D. G. Differences in Intrinsic Gray Matter Connectivity and Their Genomic Underpinnings in Autism Spectrum Disorder. *Biol. Psychiatry* **2024**, *95* (2), 175−186.
(192) Tang, Y.; Jian, M.; Tang, B.; Zhu, Z.; Wang, Z.; Liu, Y. Chiral Lanthanide Hexaazamacrocycles for Circularly Polarized Luminescence, High Relaxivity and Magnetic Resonance Imaging. *Inorg. Chem. Front* **2024**, *11* (7), 2039−2048.
(193) Yon, M.; Esmangard, L.; Enel, M.; Desmoulin, F.; Pestourie, C.; Leygue, N.; Mingotaud, C.; Galaup, C.; Marty, J. D. Simple Hybrid Polymeric Nanostructures Encapsulating Macro-Cyclic Gd/Eu Based Complexes: Luminescence Properties and Application as MRI Contrast Agent. *Nanoscale* **2024**, *16* (7), 3729.
(194) Tang, J.; Zhang, L.; Ju, Q.; Yang, F. Rare-Earth-Based Polymeric Nanobubbles as Tri-Modal Imaging Contrast Agent. *Mater. Lett.* **2024**, *363*, 136267.
(195) Marycz, K.; Smieszek, A.; Targonska, S.; Walsh, S. A.; Szustakiewicz, K.; Wiglusz, R. J. Three Dimensional (3D) Printed Polylactic Acid with Nano-Hydroxyapatite Doped with Europium(III) Ions (NHAp/PLLA@Eu^{3+}) Composite for Osteochondral Defect Regeneration and Theranostics. *Mater. Sci. Eng., C* **2020**, *110*, 110634.

https://doi.org/10.1021/acsami.4c15719
ACS Appl. Mater. Interfaces XXXX, XXX, XXX−XXX